Marine Chemistry
December 2016, Volume 187, Pages 1-15
http://dx.doi.org/10.1016/j.marchem.2016.09.003
http://archimer.ifremer.fr/doc/00350/46157/

The annual and seasonal variability of the carbonate system in the Bay of Brest (Northwest Atlantic Shelf, 2008–2014)

Salt Lesley A. [1, *], Beaumont L. [2], Blain S. [3], Bucciarelli E. [4, 5], Grossteffan E. [6], Guillot A. [7], L'Helguen S. [4], Merlivat L. [8], Répécaud Michel [9], Quéméner Loic [9], Rimmelin-Maury P. [6], Tréguer P. [4, 5], Bozec Y. [4]

[1] Sorbonne Universités, UPMC Université Paris 06, CNRS, Adaptation et Diversité en Milieu Marin (AD2M UMR7144), Station Biologique de Roscoff, 29680 Roscoff, France
[2] Division Technique INSU-CNRS, 92195 Meudon Cedex, France
[3] Sorbonne Universités, UPMC Université Paris 06, CNRS, Laboratoire d'Océanographie Microbienne (LOMIC UMR 7621) LOMIC, Observatoire Océanologique, 66650, Banyuls/mer, France
[4] Université de Brest, CNRS, IRD, UMR 6539 LEMAR, IUEM; Technopôle Brest Iroise, Place Nicolas Copernic, 29280 Plouzané, France
[5] Université Européenne de Bretagne, France
[6] UMS 3113 CNRS-UBO, Institut Universitaire Européen de la Mer (IUEM), 29280 Plouzané, France
[7] Division Technique INSU-CNRS, 29280 Plouzané, France
[8] LOCEAN, UMR 7159, CNRS-UPMC-IRD-MNHN, Univ. Paris 6, 75252 Paris Cedex 05, France
[9] IFREMER, Centre de Brest, REM/RDT/DCM, 29280 Plouzané, France

* Corresponding author : Lesley A. Salt, email address : lesley.salt@sb-roscoff.fr

Abstract :

From 2008 to 2014, the MAREL-Iroise buoy, located in the Bay of Brest, collected high-frequency measurements of partial pressure of CO2 (pCO2) and ancillary hydrographic parameters, in conjunction with a comprehensive sampling regime of two additional carbonate system variables total alkalinity (AT), and dissolved inorganic carbon (DIC). Biological processes drive variations in AT and DIC throughout the year, except in winter, when primary production is negligible and large freshwater inputs occur. Annually, the Bay of Brest generally behaves as a source of CO2 to the atmosphere (0.14 ± 0.20 mol C m− 2 yr− 1), showing inter-annual variability significantly linked to annual net community production (NCP). The presence of a large community of benthic filter feeders leads to high levels of particulate organic matter (POM) and opal deposition during the spring diatom bloom. Over the following few months, benthic POM remineralisation reduces the spring CO2 deficit relative to the atmosphere, and remineralisation of biogenic silica supplies further late spring primary production. The result is an inverse spring NCP – air-sea CO2 flux relationship, whereby greater NCP in early spring results in lower fluxes of CO2 into the Bay in late spring. This recycling mechanism, or *silicic acid pump*, also links the spring and summer NCP values, which are both determined by the peak wintertime nutrient concentrations. The carbonate system is further affected by the benthic community in winter, when CaCO3 dissolution is evident from notable deviations in the ΔAT:ΔDIC ratio. This study highlights the necessity of individual study of coastal, temperate ecosystems and contributes to a better understanding of what determines coastal areas as sinks or sources of CO2 to the atmosphere.

Highlights

► The Bay of Brest generally behaves as a source of CO_2 to the atmosphere. ► Inter-annual variability in air-sea CO_2 exchange is linked to net community production. ► Springtime net community production is determined by the winter, river dissolved silica supply. ► Total alkalinity and dissolved inorganic carbon variability is driven by biology.

Keywords : Bay of Brest, Carbonate system, Dissolved inorganic carbon, Total alkalinity

1 Introduction

The global ocean mitigates the increase in anthropogenic atmospheric carbon dioxide (CO2) through uptake and sequestration (Sabine, 2004; Archer, 2005) leading to the phenomenon known as ocean acidification (OA) (Caldeira and Wickett, 2005; Orr et al., 2005). Coastal and shelf seas support a disproportionately large amount of primary production in relation to their surface area, representing up to ~30% of oceanic primary production and ~80% of oceanic organic matter burial (Gattuso et al., 1998; Wollast, 1998). These regions thus facilitate the sequestering and export of a large quantity of atmospheric carbon making shelf seas significant in the global carbon cycle (Tsunogai, 1999; Thomas et al., 2005; Arthur and Borges, 2009). On an annual scale, the sources or sinks afforded by shelf seas are often of a similar order of magnitude to that found in the open ocean (Tsunogai et al., 1999; Quay and Stutsman, 2003; Shadwick et al., 2011; Lockwood et al., 2012, and references herein), however, the high temporal variability of these regions makes them much harder to constrain in modeling studies and thus hard to predict in future climate scenarios.

Coastal and shelf seas are very active biogeochemical environments due to the close interaction between the land, ocean and atmosphere, enabling large fluxes of carbon and nutrients between the different reservoirs (Middelburg and Herman, 2007). Anderson et al. (2005) estimate that the coastal ocean receives ~80 Tmol C yr^{-1} from terrestrial sources, of which approximately half is sequestered in shallow marine sediments, the other half being either sequestered into the ocean or released to the atmosphere. Carbonate shelves, as defined by Milliman and Droxler (1996), are responsible for 37% of global organic carbon oxidation in coastal sediments, representing ~43 Tmol yr^{-1} (Krumins et al., 2013). Furthermore, Krumins et al. (2013) estimated that there is a release of 126 Tmol yr^{-1} of dissolved inorganic carbon (DIC) from coastal benthic ecosystems, and that carbonate dissolution from shallow marine sediments contributes a further 7 Tmol y^{-1} of DIC. The majority of benthic calcium carbonate ($CaCO_3$) production takes place in shelf seas, in addition to ~20% of marine pelagic $CaCO_3$ production (Balch et al., 2005) meaning the rates of calcification can have a significant impact on both total alkalinity (A_T) and DIC (Martin et al., 2007a).

Attempts have been made to categorize coastal regions (Borges et al., 2005; Cai, 2011) according to the carbonate system dynamics and air-sea CO_2 fluxes, but there exists great heterogeneity between regions necessitating the individual study of each ecosystem. Particularly at temperate latitudes, the seasonal variability in shelf waters is great. The varying importance of different processes between seasons and external and large-scale controls make temperate, coastal regions inherently inconsistent between years (Sakamoto et al., 2008; Shadwick et al., 2011; Clargo et al., 2015). In coastal regions of the North Atlantic, the Bay of Biscay shows a seasonal range of

DIC up to 81 µmol kg^{-1} (Jiang et al., 2013), whilst on the other side of the Atlantic the Scotian shelf sees variations up to 160 µmol kg^{-1} (Shadwick et al., 2011). There exists large variability even within similar ecosystems, for example, the annual net community production (NCP) varies from 2.6 mol C m^{-2} yr^{-1} in the Gulf of Biscay (Frankignoulle and Borges, 2001) to -0.6 mol C m^{-2} yr^{-1} in the English Channel (Kitidis et al., 2012). The direction of these sources and sinks on an annual basis are often also prone to change, with a region behaving as a CO_2 source one year, and a sink the next (Schiettecatte et al., 2007; Marrec et al., 2013). Predicting the direction of the CO_2 flux per year remains a challenge, as these systems remain multifaceted and are still not fully understood.

In this study time-series data of carbonate system variables with accompanying hydrographic and nutrient data acquired from 2008 to 2014 are used to determine the driving forces affecting the carbonate system in the Bay of Brest, a temperate coastal ecosystem impacted by both river inputs and the North Atlantic Ocean surface water dynamics. The biological processes and nutrient fluxes in this region have been previously studied, demonstrating the bay's resilience to eutrophication and the importance of a *silicic acid pump* (Del Amo et al., 1997; Chauvaud et al., 2000; Rageneau et al., 2002). However, the carbonate system has remained largely understudied, yet is affected by a number of the aforementioned processes and mechanisms described in the Bay. A comprehensive understanding of the carbonate system in such a coastal ecosystem is essential with its large community of calcifying organisms potentially at risk from continuing CO_2 increases and OA.

2 Study Area

The Bay of Brest is a macrotidal estuary with two main riverine inputs from the Aulne and the Elorn (Fig. 1), the former being the dominant annual contributor. The total annual discharge from the Elorn over the 10 years varies from a minimum of 115 million cubic meters (in 2011) to a maximum of 214 million cubic meters in 2012. The Aulne annual discharge is approximately four times greater, supplying a minimum 425 million cubic meters in 2011 and a maximum 1075 million cubic meters in 2014. Both rivers follow a seasonal pattern, with higher rainfall and flow rates in winter compared to summer, however, the range is much greater in the Aulne, where average flow rates drop from ~50 $m^3 s^{-1}$ in winter, to ~3 $m^3 s^{-1}$ in summer. The Elorn, in contrast falls from flow rates of ~10 $m^3 s^{-1}$ in winter to ~2 $m^3 s^{-1}$ in summer. As such, the ratio of freshwater input from each river varies throughout the year (from approximately 5:1 in December to 2:1 in September). At times of high flow, the transit time of freshwater through the Bay of Brest is a number of days (Tréguer et al., 2014). Further water exchange takes place with the North Atlantic, via the Iroise Sea.

The Bay of Brest is not sufficiently deep (average depth of ~8m) to support neither permanent nor seasonal stratification. Temporary stratification can occur in some regions during neap tides or saline stratification during times of large freshwater input, however, the influence of tides generally maintains a well-mixed water column all year round, as seen from the numerous CTD profiles made by the SOMLIT observatory over the past decade (available at http://somlit-db.epoc.u-bordeaux1.fr/bdd.php). Large inputs of nutrients from both rivers facilitate substantial primary production in spring and summer. The annual succession of phytoplankton

starts in mid-February, with increases in microphytoplankton, and by early march diatoms start to dominate (Del Amo et al., 1997); prevalent in the >10 µM size class. This initial spring bloom peaks in mid- to late-April, and the following post-bloom phytoplankton community continues to see a dominance of diatoms until late summer (August-September), at which point nanophytoplankton become the dominant species for the last autumn bloom period (Quéguiner and Tréguer, 1984; Del Amo et al., 1997). Large variability in this succession has been observed between years, and is largely dependent upon the climatic conditions, particularly the river contribution of nutrients (Le Pape et al., 1999). Despite this, overall, diatoms represent ~73% of the annual integrated primary production (Del Amo et al., 1997).

Furthermore, there is a large community of suspension benthic-feeders in the Bay of Brest, dominated by *Crepidula fornicata L.* (slipper limpet), a benthic gastropod, covering approximately half of the floor of the Bay (Chauvaud et al., 2000), and a large community of *Maerl* dominating roughly one third of the benthos in the shallower environments (Ni Longphuirt et al., 2007). It has been calculated that the microphytobenthos represents up to 20% of the known total production (pelagic and benthic) in the Bay of Brest (Ni Longphuirt et al., 2007). The particular species abundant in the Bay of Brest (*C. fornicata*), is also a calcifying organism and has been shown to perform the majority of respiration in the benthic community in addition to calcium carbonate production (Martin et al., 2006).

3 Data and Methods

3.1 Data collection

From 2008 to 2014, hourly measurements of the partial pressure of CO_2 (pCO_2) and temperature of seawater were made using a CARIOCA sensor, which is installed on the MAREL-Iroise buoy, located at 48.35° N, 4.55°W (Fig. 1)(managed according to the terms of the framework agreement jointly signed by IFREMER, CNRS (INSU) and UBO on behalf of IUEM (no 11/2-210922)). The measurement of pCO_2 follows the colorimetric method outlined in Lefèvre et al. (1993), whereby the CO_2 in seawater equilibrates with the pH-sensitive thymol blue dye across a semi-permeable membrane. The color change in the dye is monitored by measuring the absorbance of three wavelengths in the cell and the pCO_2 is calculated from the pH change measured in the dye. The precision of the CARIOCA pCO_2 measurements has been estimated at ±1 µatm (Boutin et al., 2009) with an accuracy of 3 µatm. Over the total period of deployment two CARIOCA sensors have been used, on a three-month rotation. The MAREL-Iroise Buoy performs ancillary measurements of temperature, conductivity, dissolved oxygen (DO), fluorescence and photosynthetically active radiation (PAR) every 20 minutes at a depth of 2.5 m (for more details we refer the reader to Blain et al., 2004 and http://conference-marelcarnot2014.fr/Presentations_files/Presentation-Rimmelin.pdf). These sensors have a precision of 0.05ºC, ±0.05 ms cm^{-1}, ±5%, ±5% and ±3 µE m^{-2} s^{-1}, respectively. The oxygen saturation level (DO%) was calculated according to Weiss (1970) from the observed DO and the DO at saturation using the *in-situ* temperature and salinity data.

In addition to autonomous measurements, discrete bottle samples were collected using a Niskin bottle, from a location about 100m away from the buoy, every week at the

SOMLIT (Service d'Observation du Milieu LIToral) Brest sampling station (48.36°N, 4.55°W) (Fig. 1). SOMLIT-Brest is part of the French network for monitoring of the coastal environment (SOMLIT, http://somlit.epoc.u-bordeaux1.fr/fr), INSU-CNRS. It provides more than 20 core-parameters of the marine environment collected at 2 m depth, at high tide, every week. For this study we used the discrete weekly measurements of chlorophyll-*a* (Chl-*a*) and inorganic nutrients (nitrate (NO_3^-), silicic acid ($Si(OH)_4$) and phosphate (PO_4)) collected during the deployment of the CARIOCA buoy.

Chlorophyll samples were taken in opaque bottles, which were rinsed three times with sample before sampling. 0.5 L of seawater were filtered through glass-fibre filters (Whatman GF/F) and immediately frozen. Samples were extracted in 5 mL of acetone. Correction for phaeopigments was carried out using the acidification method with a HCl solution, after primary fluorescence measurements using a fluorometer (Turner Designs model 10 AU digital fluorometer) to calculate Chl-a concentrations according to EPA (1997). The estimated accuracy was 0.05 μg L^{-1}.

Samples for the analysis of the inorganic nutrients nitrate, silicic acid and phosphate, were taken from the Niskin using tygon tubing into 150 ml bottles. Samples were then stored at -20ºC or analysed immediately using an AA3 auto-analyser (AXFLOW) following the method of Aminot and Kerouel (2007) with accuracies of 0.02 μg L^{-1}, 1 ng L^{-1}, 1 ng L^{-1}, and 0.01 μg L^{-1} for NO_3^-, NO_2^-, PO_4^{3-} and SiO_4^-, respectively. Further details on the analytical techniques used for each parameter can be found in Bozec et al. (2011).

During the same period, additional samples for A_T and DIC were collected weekly at the SOMLIT-station, following the recommended procedure (Dickson, 2007). Subsamples from the Niskin bottle were tapped into 500 ml borosilicate bottles using tygon tubing. Bottles were filled and overfilled twice to minimize gas exchange between the sample and the air. Samples were poisoned with 300 µg of $HgCl_2$, stopped with greased stoppers and the lids held tight using elastic bands, and stored in the dark at ~4°C prior to analysis. From 2008 to 2012, DIC and A_T were measured simultaneously by potentiometric titration derived from the method developed by Edmond (1970) using a closed cell at the national facility for analysis of carbonate system parameters (SNAPO-CO_2, LOCEAN, Paris). The calculation of equivalence points was done using a non-linear regression. From 2012 analyses were performed on a VINDTA 3C at the Roscoff laboratory. For both techniques certified reference material (CRM), supplied by Prof. Andrew Dickson (Scripps Institute of Oceanography, UCSD La Jolla, CA) were run at periodic intervals for quality control. Measurements of CRM indicates that the accuracy of our measurements of A_T and DIC were 3 and 2 µmol kg^{-1}, respectively (for further details see Marrec et al., 2014). pH was computed from DIC and A_T measurements as explained in section 3.3.

The climatologies, for the period 2008-2014, are shown in Fig. 2. These were calculated by first binning all the data per month to obtain average values for each month of each year, and then averaging these monthly values to calculate the climatology. For the high-frequency measurements (salinity, temperature, dissolved oxygen, pCO_2) the data were first binned per hour, and then per day. In this way any

diurnal-bias in the data is minimized. Furthermore, only months with a minimum of 10 days of data were used, to ensure that the values are representative.

The station Roscanvel is also shown in Fig. 1, where rates of dissolution/production of $CaCO_3$ were measured from March 2002 to October 2004 by *in-situ* incubation experiments and using the alkalinity anomaly technique (Martin et al. 2007a).

3.2 Calculations

3.2.1 Air-Sea CO_2 flux calculations

Thermodynamics drives the flux of CO_2 between the ocean-atmosphere boundary with the direction of the flux going from high to low concentration. In the ocean this is a turbulent process, strongly influenced by wind speed. The air-sea flux of CO_2 was calculated following Eq. 1.

$$F = k \cdot K_0 \cdot (pCO_2^{sea} - pCO_2^{air}) \qquad \text{[Eq. 1]}$$

where k is the gas transfer velocity of CO_2, K_0 is the solubility coefficient, and pCO_2^{sea} and pCO_2^{air} are the partial pressure of CO_2 in the surface layer and atmosphere, respectively. Here, we apply the gas transfer velocity of CO_2 of Nightingale et al. (2000), with monthly averaged wind speed data, corrected to 10m height, and obtained from the ERA-Interim project (Dee et al., 2011). Both the gas transfer velocity of Nightingale et al. (2000) and the wind speeds from the ERA-Interim project have been shown to be the preferred choices in the adjacent Bay of Biscay (Otero et al., 2013). The atmospheric pCO_2 (pCO_2^{air}) was computed from the

mole fraction of CO_2 (xCO_2) measured at Mace Head, Ireland (RAMCES network; Observatory Network for Greenhouse Gases), and corrected for water vapor pressure, following Weiss and Price (1980), and to the atmospheric pressure in the Bay of Brest, obtained from the ERA-Interim reanalysis project (Dee et al., 2011). Mace Head is the closest, long-term source of atmospheric CO_2 data in the vicinity of our study region. Its distance to the Bay of Brest may lead to variations in concentration between the two locations, however, as the prevailing winds in the Bay of Brest are northwesterly, the potential bias in atmospheric CO_2 concentration at the two sites remains minimal.

3.2.2 NCP calculation

To obtain an estimate of net community production (NCP = TP – CR) in the Bay of Brest on an annual and seasonal scale, we used the equation of Sarmiento and Gruber, (2006).

$$dDIC/dt = dDIC/dt\,|_{EX} + dDIC/dt\,|_{NCP} + dDIC/dt\,|_{TRSP} + dDIC/dt\,|_{DIFF} \ldots + dDIC/dt\,|_{ENT} \qquad \text{[Eq. 2]}$$

The original (Eq. 2) describes the changes in DIC caused by the biological processes of photosynthesis and remineralisation (NCP), the effects of air-sea gas exchange of CO_2 (EX), horizontal and vertical advection (TRSP), horizontal and vertical diffusion (DIFF), and vertical entrainment from the mixed layer (ENT). As the Bay of Brest is not deep enough to support a mixed layer, terms for vertical entrainment and diffusion were omitted. We also do not consider any flux at the sediment-water interface, as the benthic environment is well oxygenated, any fluxes would be generated by the same

processes ongoing in the pelagic environment (e.g. photosynthesis, respiration). However, this does mean that later we cannot differentiate between the NCP term in the benthic versus the pelagic compartment. The consistent DIC-salinity wintertime mixing line indicates that the impact of the advected river water into the Bay of Brest will be dominant over any changes to the North Atlantic end member, so we use this wintertime DIC-salinity regression to account for the advection term. Changes to the seasonal end member values of the North Atlantic input, via the Bay of Biscay and Iroise Sea, are very difficult to predict. We assume that the seasonal changes are of a similar scale to that observed in the Bay of Brest (although they are likely to be smaller; Jiang et al., 2013) and thus the signal measured in the Bay of Brest remains representative of the adjacent Iroise Sea. The air-sea CO_2 flux was calculated from pCO_2 data from the CARIOCA buoy (Methods 3.2). These monthly-averaged calculated values were then substituted in the rearranged Eq. 2:

$$dDIC/dt - dDIC/dt\,|_{EX} - dDIC/dt\,|_{TRSP} = dDIC/dt\,|_{NCP} \qquad \text{[Eq. 3]}$$

The resolved monthly $dDIC/dt|_{NCP}$ term is the sum of the change in DIC attributed to calcification/dissolution and primary production/respiration. A negative term is indicative of primary production (PP), or uptake of DIC and calcification, whereas a positive value indicates remineralisation and dissolution. As such, when NCP is discussed, the inverse term is used, as a positive NCP is indicative of autotrophy and a negative NCP indicative of heterotrophy. The errors of each individual term of equation 3 were propagated to estimate the uncertainty of $DIC|_{NCP}$ to 16 µmol kg^{-1}. Additionally, as mentioned, the resultant NCP calculated here is representative of combined benthic and pelagic processes.

Similar to DIC, A_T is conservative with regards to temperature and salinity and is also modified by biological processes, such as, PP, $CaCO_3$ production/dissolution and the uptake and release of nutrients during organic matter production (OMP) (Brewer and Goldman, 1976; Chen, 1978). The pelagic environment in the Bay of Brest remains well oxygenated all year round, thus we did not consider the benthic anoxic processes, which can effect A_T, such as, denitrification and sulfate reduction. Furthermore, A_T is not affected by air-sea gas exchange of CO_2, thus the equation to describe changes to A_T can be simplified to Eg 4:

$$dA_T/dt = dA_T/dt|_{TRSP} + dA_T/dt|_{OMP} + dA_T/dt|_{CaCO3} \qquad \text{[Eq. 4]}$$

3.3 The internal consistency of the carbonate system

The measurements of more than 2 carbonate parameters allows us to compare how well our measurements match up to values calculated from equilibrium relationships. Calculations were performed using the CO2SYS program (Lewis and Wallace, 1998) and the carbonic acid dissociation constants of Millero et al. (2006), which have been shown to be the most robust in coastal areas of varying salinity (Salt et al., 2015). Further, the KSO_4 dissociation constant of Dickson (1990) was used along with in situ temperature, salinity and nutrient concentrations, and pH values are reported on the total scale. The pCO_2 values were matched with the DIC and A_T sample with the smallest time difference, up to a limit of 4 hours difference. For 95 of the samples there was a DIC and A_T sample corresponding to within 20 minutes of the pCO_2 measurement, for 127 samples there was a pCO_2 measurement within the hour, and for 7 pCO_2 measurements there was a pCO_2 measurement within 4 hours. Thus we

could assess the internal consistency for 229 points. This represents 78% of the A_T and DIC data, but less than 1% of the pCO_2 data.

The average difference between the measured and calculated values were of a similar scale to that presented in other studies of the carbonate system in coastal regions (Salt et al., 2015; Ribas-Ribas et al., 2014). When regressed against the measured respective values, we could predict A_T to ±7 µmol kg^{-1}, DIC to ±6 µmol kg^{-1}, and pCO_2 to ±33 µatm. Of these total errors, the analytical errors carried through from input parameters contributes a variability of ±4 µmol kg^{-1} to A_T, ±3 µmol kg^{-1} to C_T, and ±12 µatm to pCO_2. It is possible that a further fraction of this inconsistency is based in spatial heterogeneity between the two sites (100m apart). However, from these reasonable results, we are confident that combining the dataset of DIC and A_T with the high-frequency pCO_2 observations, results in a sufficiently consistent dataset of all three carbonate variables. The pH results discussed here, as well as the aragonite and calcite saturation states (ΩAr, ΩCa), are the results of the pH calculated using DIC and pCO_2 as input parameters, which has been shown to be the more robust pairing for calculating pH (Salt et al., 2015).

4 Results

4.1 Annual cycle of inorganic nutrients and phytoplankton

The calculated climatology of salinity, temperature, Chl-*a*, DO%, pH, pCO_2, NO_3^-, $Si(OH)_4$, A_T and DIC measurements at 2m depth are shown in Fig. 2, with the variability shown as one standard deviation (s.d.) of the mean. The climatological

means are calculated from 7 years of observations (January 2008 – January 2015). From hereon in, spring refers to yeardays 60 – 151 (March – May), summer includes yeardays 152 to 243 (June – August), autumn includes yeardays 244 to 334 (September – November), and winter includes yeardays 335 to 59 (December – February).

Fig. 2a shows the typical annual pattern of temperature and salinity, with a distinct seasonality, typical of coastal, temperate regions of northwestern Europe. The temperature and salinity values both peak in August, when air temperatures are highest and river runoff is lowest, with a minimum in temperature and salinity following in February. Temperatures in the Bay of Brest ranged from 7.4°C in winter (minimum in 2010) to 18.3°C in summer (maximum in 2012), and demonstrate a low level of inter-annual variability (months show a variability of <±1°C, or <8% of the range). The average salinity remains quite high at 34.5 throughout the 7 years, thus seawater (North Atlantic water) is consistently the dominant water mass present (Table 1). Over the past 7 years salinity values range between 32.4 and 35.5, with distinct peaks and troughs closely linked to local river discharge (Fig. 3). The salinity shows a much greater intra- and inter-annual variability than temperature, with winter months showing an average standard deviation (s.d) representative of 28% of the range of the past 7 years.

The annual signal of inorganic nutrients (NO_3^- and $SiOH_4$) show strong seasonality linked to both river discharge and biological processes (primary production, remineralisation) in the area (Fig. 2). Wintertime peaks in NO_3^-, and $SiOH_4$ are

observed on the same day and coincide with maximum river discharge (Fig. 3), the latter of which occurs consistently between mid-January and early March for all observed years. Following this peak, inorganic nutrients show decreasing concentrations from February to July as Chl-*a* increases, reflecting biological uptake. The climatology indicates a concomitant decrease in NO_3^- and $SiOH_4$ from spring to an early summer minima in June/July. However, whilst this is accurate for 2010, and 2011, in the majority of years, on a finer timescale, the $SiOH_4$ concentration actually demonstrates a double-dip, in spring and summer (Fig. 3). The first trough (excepting 2009), represents the annual $SiOH_4$ minima and results in $SiOH_4$ near-, or total, exhaustion, with concentrations <1 µmol kg^{-1} (on yeardays 90, 79, 125, 93, 75 and 101 for the years 2009, 2010, 2011, 2012, 2013 and 2014, respectively). However, the second, smaller trough coincides with NO_3^- exhaustion and does not result in $SiOH_4$ exhaustion. This NO_3^- exhaustion occurs on yeardays 149, 168, 132, 107, 170 and 153 in 2009, 2010, 2011, 2012, 2013 and 2014, respectively.

4.2 Annual cycle of the carbonate system

The annual pCO_2 distribution is closely tied to the phytoplankton dynamics and thus mirrors the Chl-*a* signal quite closely (Fig. 2b). The annual range in pCO_2 values varies from 400 µatm (range 219 – 620 µatm) in 2010 to 603 µatm (range 284 – 888 µatm) in 2014 (not shown). Between years, the wintertime pCO_2 shows great variability (Fig. 3d) with the maximum observed range of 606 µatm being almost equal to the entire annual range of 603 µatm in 2014. There is a substantial decrease in pCO_2 between the end of winter and the onset of the spring bloom, each year, with values decreasing on average 196 ± 79 µatm during the spring season (Fig. 2c). The

peak in Chl-*a* coincides with the pCO_2 minimum in May, indicating that the spring phytoplankton bloom is the driving force behind this pCO_2 decrease (Fig. 2b,c). After this peak in May, the Chl-*a* concentration decreases and pCO_2 increases again. Similarly, photosynthesis leads to large decreases in DIC, as well as pCO_2, from March to June. However, there is a marked decoupling of DIC from pCO_2 around June, when pCO_2 values reach a minimum while DIC values continue to decrease. Despite the increase in pCO_2 through summer, concentrations stay below atmospheric levels until August, at which point they surpass atmospheric CO_2 equilibrium and continue to increase to peak values in October.

The annual pattern of DIC reflects that of the inorganic nutrients, demonstrating the preponderant influence of biologically driven processes on the carbonate system. The DIC shows a single peak in November followed by gradually decreasing values through winter and spring to a minimum in July (Fig. 2f). This pattern is consistent for all years, although there is a low level of variability on a finer time scale (Fig. 3e). For each of the years measured, the DIC annual range remains between 2000 – 2150 µmol kg^{-1}. The annual range in 2011 and 2014 are slightly below the other years, but overall years of observations show comparable behavior. For all years, the seasonal amplitude of DIC is almost double that of total alkalinity (A_T). Further in contrast to DIC, there is an annual double-peak distribution of A_T present for all years, with the first peak occurring at the end of spring (June) and the second peak towards the end of summer (September). This is most evident in the climatology (Fig. 2f), however, less pronounced in the time series (Fig. 3e) due to a smaller signal to noise ratio. The two peaks are also less distinct in 2013 and 2014, compared to the previous four years. This double peak corresponds approximately to the first and second peaks seen in

Chl-*a* concentration, however, the comparative sizes of the two peaks are not proportional (Fig. 3(c)(e)).

The two main rivers (Elorn and Aulne) contributing to the Bay of Brest show low zero-salinity end member concentrations of DIC and A_T (measured in the respective estuaries from 09/02/2009-10/02/2009 for winter, 18/05/2009 – 19/05/2009 for spring, 01/07/2009 – 02/07/2009 for summer and 12/11/2009 – 16/11/2009 for autumn; data not shown, available in Bozec et al., 2011) compared to the North Atlantic, which is responsible for the majority of the water budget in the Bay of Brest (Table 1). During winter, across all years, salinity shows a remarkably constant linear relationship with DIC, with a Pearson correlation coefficient of 0.80 (p-value: <0.005) (Fig. 4a). There is greater scatter in the data at the lowest salinities, which correspond to the high river flow rates found in the winter of 2013/14. The winter of 2013/14 experienced exceptionally high rainfall. Tréguer et al. (2014) showed that large-scale hydro climatic indices such as East Atlantic Pattern (EAP), and weather regimes such as the Atlantic Ridge (AR) have a major influence on precipitation, which in turn modify river discharge that impact surface salinity at the SOMLIT-Brest site (dilution effect) and thus might be responsible for the scatter. Seasonal data from the rivers Elorn and Aulne (Table 1) indicate that the seasonal DIC end member in the two rivers is minimal. If we extrapolate the difference caused by this end member seasonality to the average salinity recorded in the Bay of Brest during the time series, this introduces a maximum variability in DIC contributions of 7 μmol DIC kg^{-1} from the Elorn and 3 μmol DIC kg^{-1} from the Aulne, allowing us to calculate the estimated wintertime DIC to within ±10 μmol kg^{-1}. The best fit line of salinity and DIC,

including the wintertime end members (Table 1) is used to calculate the $DIC|_{TRSP}$ term in Equation 3.

Like the DIC-salinity relationship in winter, the wintertime values of salinity and A_T demonstrate a significant linear relationship (Fig. 4b), which remains constant throughout the years, with a Pearson correlation coefficient of 0.81 (p-value: <0.005), with fresher waters having a lower A_T value. The zero-salinity end members of A_T in the two rivers shows a similar level of variability to that observed in DIC (Table 1), with the greatest seasonal difference being 48 µmol A_T kg^{-1} in the Aulne and 134 µmol A_T kg^{-1} in the Elorn. Seasonal variation from riverine contributions would thus contribute, on average, a variability of up to 9 µmol A_T kg^{-1} from the Aulne, and 4 µmol A_T kg^{-1} from the Elorn. Seasonal variations show that concentrations of DIC are highest, in both rivers, during autumn and winter, and lowest in spring. In contrast, A_T values are highest in the Elorn in winter, and lowest in spring, however, in the Aulne, A_T values are highest in spring and summer, and slightly lower in autumn and winter. A similarly linear relationship is found in winter between NO_3 - salinity and $SiOH_4$ – salinity (Tréguer et al., 2014).

4.3 Net community production (NCP)

To estimate the NCP in the Bay of Brest we used the wintertime DIC-salinity relationship (including winter river end members; Table 1) to account for advective transport (as biology in winter is negligible; Treguer et al., 2014) and the calculated air-sea flux of CO_2 to account for changes in DIC from month to month (section

3.2.2). Solving this for monthly-averaged values of DIC we calculate annual and seasonal NCP in the Bay of Brest (Table 2). The relative contributions of each factor influencing DIC (Fig. 6) indicates that NCP, advective transport and air-sea gas exchange of CO_2, all play similarly significant roles on a month-to-month basis. In spring both NCP and transport exert a diminishing influence on DIC, whereas the gas exchange with the atmosphere exerts a positive contribution. As of May, NCP starts contributing positively to DIC, indicating that the Bay of Brest has switched from an autotrophic to a heterotrophic dominated system. As DIC starts to show an overall increase at this time of year, NO_3^- concentrations are still decreasing, indicating preferential recycling of nutrients (Thomas et al., 1999). Two months after this, in July, the effect of air-sea gas exchange reverses and exerts a diminishing effect on DIC, indicative of outgassing. The presence of CO_2 outgassing at this time of year is in line with the observations of seawater CO_2 (Fig. 2c), which rise to atmospheric levels at this time of year.

The NCP was also calculated using the change in NO_3 concentration and the Redfield ratio (NCP_{NO3}). These calculations show a significant correlation (r=0.88, p-value = 0.005) with the NCP calculated using DIC, however, the NCP_{NO3} values are significantly larger than the former values, by 0.3 to 0.8 mol C m^{-2}. When river flow into the Bay of Brest is notably large, the transit time of the water through the Bay is much faster (of the order of days; Treguer et al., 2014), thus high nitrate concentrations in the Bay derived from riverine sources may not all be used within the Bay, but may exit the Bay, into the North Atlantic, unconsumed. Post spring, there is also a high degree of OM turnover in the bay. As such, a significant proportion of the carbon taken up is likely to be re-released back into the water column, resulting in an

overall lower NCP and accounting for the difference between carbon-derived NCP and nitrate-derived NCP. For further considerations, we use the NCP_{DIC} calculations for consistency with the air-sea CO_2 flux values.

When considering the changes to A_T in the bay, it is principally the changes driven by advection and biology to consider. Again, we use the wintertime A_T-salinity regression (including end member values) to account for advection and deduce that the remaining changes are driven by biological processes (see section 3.2.2). The only way to differentiate between the $dA_T/dt|_{CaCO3}$ and the $dA_T/dt|_{OMP}$ component, is by assuming that the $dA_T/dt|_{OMP}$ is caused by nitrate uptake and thus calculate this fraction from changes in nitrate concentration. Uptake of 1 mole of NO_3^- by phytoplankton results in an increase in A_T of 1 mole. Fig. 7a shows the advective component $A_T|_{TRSP}$ alongside the observed values, with the difference ($dA_T/dt|_{OMP}$) shown in Fig. 7b, with the NO_3^- concentration.

Fig. 7a shows an expected peak in $A_T|_{TRSP}$ in late summer, when river flow is at a minimum and the high A_T waters of the North Atlantic are more prevalent. However, there is a smaller peak in $A_T|_{OBS}$ in April before that, which is not explained by salinity changes. From Fig. 7b we can see that there is a clear source of A_T in the Bay of Brest from mid-winter until the end of spring. The source of A_T is present at the same time of year as NO_3^- uptake, indicating a link between the two, however, both A_T and NO_3^- appear to decrease simultaneously during later spring. After the initial spring bloom, when OM is broken down, the remineralised nitrogen can be broken down into ammonia or nitrate; the former increasing A_T and the latter decreasing A_T.

Phytoplankton may take up ammonia or NO_3^- for OMP, the former decreasing and increasing alkalinity by 1 mol, respectively. The proportions of these processes cannot be deduced from the measurements available, and thus we do not attempt to use AT_{NO3} beyond the Spring season. The oscillation from source to sink maintains a relatively constant amplitude (±30 µmol kg^{-1}) from year to year, with the one exception of the winter of 2013/14.

4.4 Air-Sea CO_2 fluxes

Seasonally calculated air-sea CO_2 fluxes reveal that the Bay of Brest behaves as a sink for atmospheric CO_2 during spring and summer but emits CO_2 to the atmosphere during autumn and occasionally during winter (Fig. 8). The Bay remains relatively neutral during winter, and summer compared to the other seasons, with respective average total seasonal fluxes of 0.06 and -0.03 mol C m^{-2}. On an annual basis, for the study period (2008 to 2014), the Bay of Brest behaves as an overall source of CO_2 to the atmosphere, with an average annual flux of +0.14 (±0.20) mol C m^{-2}. The annual fluxes range from a minimum value of -0.17 mol C m^{-2} in 2009 to a maximum annual source of +0.38 mol C m^{-2} in 2013. The total springtime (March – May) CO_2 fluxes range from -0.29 mol m^{-2} in 2010, to 0.05 mol C m^{-2} in 2013. Most efflux of CO_2 is observed during autumn, and ranges from 0.13 mol C m^{-2} in 2010 to 0.30 mol C m^{-2} in 2013. Wintertime fluxes demonstrate greater variability, with the maximum flux (0.31 mol m^{-2} in 2014) in the same range as the autumn max and the minimum flux (-0.11 mol m^{-2} in 2008) being of a similar order of magnitude to the springtime fluxes. During winter there is also greater day-to-day variability in the fluxes, reflecting the degree of variability seen in the pCO_2 observations (Fig. 3d).

5 Discussion

5.1 The effects of the *Silicic-acid Pump* on NCP

The annual supply of inorganic nutrients into the Bay of Brest is largely controlled by river supply. A recent analysis by Tréguer et al. (2014) found that river runoff into the Bay of Brest is significantly positively correlated to the large-scale teleconnection indices of the East Atlantic Pattern and negatively related to the Scandinavian Blocking weather regime. We observe that the $Si(OH)_4$ and NO_3^- concentrations decrease with flow, which has been observed by Tréguer et al. (2014), and Quéginer and Tréguer (1986), and explains why both nutrient concentrations peak simultaneously over the 7 years. Looking solely at the wintertime inorganic nutrient delivery to the Bay we see that the ratio of $SiOH_4$ to NO_3^- remains relatively constant compared to the $SiOH_4$ to PO_4 ratio, with fluctuations in the former ranging from 0.2:1 to 0.5:1 between the years.

The phytoplankton succession in the Bay of Brest has been well documented (Del Amo et al., 1997; Le Pape et al., 1999, Chauvaud et al., 2000), with diatoms dominating from the spring bloom to September. By plotting NO_3^- against $Si(OH)_4$ concentrations for each year (not shown) during this first period of decline in $Si(OH)_4$ (February – April), and regressing a straight line (where $SiOH_4$ is on the *x*-axis) through the data, the location at which the line crosses each axis gives an indication of which nutrient was exhausted first, and thus whether the system was limited by NO_3^- or $Si(OH)_4$. The intercept on the *y*-axis is positive for all years, except in 2011, when

both nutrients reach exhaustion at a similar time (intercept (0,0), on yearday 125). These result indicate $Si(OH)_4$ -limitation, which is in line with previous findings (Le Pape et al., 1999). Following the depletion of $Si(OH)_4$ there is a subsequent short-term period of $Si(OH)_4$ remineralisation, which raises $Si(OH)_4$ levels to approximately a third of their pre-bloom value. Fig. 9a and 9b show the relationship between NCP and winter $Si(OH)_4$ and NCP and winter NO_3^-, with two different linear relationships; the summer gradients significantly shallower than the spring gradients. The summer relationship shows a linear correlation with negative values of NCP (in contrast to the positive NCP values observed in spring), indicative of a predominance of OM remineralisation. As such, this suggests that the initial bloom – determined by peak winter $Si(OH)_4$ concentrations - plays a significant role in controlling the NCP balance in the subsequent season, which also explains the presence of a significant linear correlation between the NCP_{spring} values and NCP_{summer} values (Fig. 9d). The summer air-sea CO_2 flux is no longer correlated to NCP_{summer} as physical factors (e.g. temperature) exert a stronger influence (Fig. 9c).

The recovery of the Bay of Brest from $Si(OH)_4$ exhaustion in spring is due to the *silicic acid pump* in the Bay of Brest (Del Amo, 1997; Chauvaud et al., 2000; Ragueneau et al., 2002; Ragueneau et al., 2005). This term was coined to describe how, following the end of the first spring diatom bloom, the majority of OM is not remineralized in the pelagic zone, but is rapidly transported to the seafloor via biodeposition, due to the presence of large macrozooplankton and benthic feeders. Biodeposition in beds of suspension-feeding mollusks results from the active filter feeding by a mollusk, which leads to non-digested material being excreted to the sediment surface as feces and pseudo-feces. Mollusks, therefore, strongly affect

physical, chemical and biological properties near the sediment–water interface. In particular, this process typically result in local deposition rates that exceed that of passive physical sedimentation.

During springtime the ratio between BSi dissolution rates and production rates is at its lowest (0.37; Beucher et al., 2004), thus leading to a build-up of diatoms in the pelagic zone. The amount of biodeposition of BSi is controlled by the benthic population and the time taken for the recycling of the deposited BSi in the Bay of Brest is of the order of one month (Le Pape et al., 1999), thus the BSi from the spring bloom would be released over the subsequent season (spring-summer). Ragueneau et al. (2002) calculate that in early spring, riverine nutrient supplies provide 100% of the demand for $Si(OH)_4$, however, already by late spring this has fallen to 30%, with the remaining 70% made up by benthic recycling. In mid-summer, the benthic flux is estimated to be sufficient to meet 100% of the silicate demand. The presence of this pump explains why we observe significant correlations between both NCP_{spring} and NCP_{summer} and the wintertime $Si(OH)_4$ concentrations. The level of production during the first spring bloom is directly related to the supply of nutrients to the Bay of Brest via the rivers, and the OMP taking place in the subsequent season (summer) would be directly related to the amount of biodeposition from the initial bloom.

The aforementioned influence of teleconnection patterns on the river runoff (Tréguer et al., 2014) influences directly the supply of $Si(OH)_4$ and NO_3^- into the Bay of Brest (Quéginer and Tréguer, 1986). We show here that this wintertime $Si(OH)_4$ concentration is the primary control of NCP_{spring} and subsequently NCP_{summer}. The

NCP_{spring} values also show a clear relationship to air-sea CO_2 flux at this time of year, which exerts a significant impact on the annual flux relationship. This shows a direct impact between large-scale teleconnection patterns and CO_2 uptake on a local scale. These relationships are robust and contribute significantly in explaining a fraction of the large variability, in magnitude, and sign, of NCP in the Bay of Brest, and potentially, other coastal systems. Furthermore, it has previously been suggested that the *silicic-acid pump* controls the effects of eutrophication in the Bay of Brest, by maintaining diatom dominance all year round (Del Amo et al., 1997). This prevents low $Si(OH)_4$:NO_3 ratios developing – as per usual in nitrogen enriched waters – and thus the Bay has a degree of protection from eutrophication. It is likely this same mechanism would control the Spring and post-Spring NCP and thus the air-sea CO_2 flux at this important time of year.

5.2 The carbonate system in the Bay of Brest

Previous studies examining controls on the carbonate system in coastal and shelf seas have largely relied upon multi-annual, low-frequency data (Jiang et al., 2013; Marrec et al., 2013; Salt et al., 2013; Clargo et al., 2015), or high-frequency data collected over short time periods (Bozec et al., 2011; Shadwick et al., 2011). Here we combine the two approaches to give a thorough analysis of the controls of the carbonate system in the Bay of Brest.

Throughout the study period, both A_T and DIC demonstrate a closely coupled relationship (Figure 4). The dominant annual processes affecting the carbonate system

in the Bay of Brest, and their stoichiometric influence on A_T and DIC, are shown in Fig. 5a; being OM production and remineralisation, calcium carbonate ($CaCO_3$) production and dissolution, and air-sea gas exchange. Photosynthesis and OM production, under Redfield conditions, results in a decrease in DIC of 106 moles and an increase in A_T of 17 moles (Brewer and Goldman, 1976) per mole OM produced. The change in A_T is approximate as it depends on the chemical species of nitrogen used (Wolf-Gladrow et al., 2007) and it assumes accordance to fixed Redfield ratios although these are known to vary between different phytoplankton taxonomic groups (Schoemann et al., 2005). The reverse reaction asserts the opposite impact, although the sole dominance of either of these reactions would result in a ratio of ~0.16:1 between ΔAT:ΔDIC. Calcification - the process of forming calcium carbonate from calcium ions and bicarbonate ions or carbonate ions - acts to decrease alkalinity by 2 moles per mole of $CaCO_3$ formed. Figure 5a sees a shift from a steep winter slope (ΔAT:ΔDIC of 1.2:1), to a notably lower ratio (0.36:1) in spring, which reaches the minimum (0.26:1) in summer (Fig. 5a). This pattern is reversed as the year proceeds through autumn (0.36:1), returning to the annual maximum (1.2:1) in winter again. The ratio of ΔAT:ΔDIC in the river end members has annual variability ranging from 0.75 – 0.85 in the Aulne and from 0.85 to 0.94 in the Elorn (Table 1), which are insufficient to account for the observed seasonal changes in the Bay of Brest. Given the complexity of the systems, we examine the processes dominating in the Bay per season and summarize the main findings at the end of the section.

In wintertime biological activity is negligible, demonstrated by conservative mixing lines of NO_3^- and $SiOH_4$ (Tréguer et al., 2014), and we have shown A_T and DIC behave in a similar conservative manner (Fig. 4); the A_T and DIC display a significant

linear relationship to each other, with a Pearson's correlation coefficient of 0.94 (*p*-value < 0.005) (A_T = 1.2 DIC). The decreasing A_T and DIC at this time of year (Fig. 5a) is largely driven by freshwater inputs. However, given the higher winter ratio of ΔAT:ΔDIC compared to the river end member variability, a degree of $CaCO_3$ dissolution must be on-going. Martin et al. (2006) observed maximum dissolution rates of 4 µmol $CaCO_3$ g^{-1} ash free dry wt. h^{-1} in *Crepidula fornicata* L. populations during winter at Roscanvel station (Fig. 1), which explains the higher ΔAT:ΔDIC observed at this time of the year. Also, winter in the Bay is characterized by minimum A_T values and maximum DIC values, resulting in the annual minimum pH values (<8.05) (Fig. 2c) and the lowest calculated saturation state of aragonite (ΩAr) (<1.5). While the aragonite saturation state remains supersaturated within the water column, it is likely that the benthic environment experiences localized undersaturation due to the release of CO_2 to pore waters during benthic OM degradation (Jahnke et al., 1997).

From winter to spring A_T increases and DIC decreases resulting in an ΔAT:ΔDIC ratio decrease from 1.2 to 0.36 (Fig. 5). This implies a dramatic shift to a greater proportion of OM production taking place compared to $CaCO_3$ production/dissolution. At this time of year, primary production is occurring at the annual maximum rate ~218 mg C m^{-3} d^{-1} (Del Amo et al., 1997) and calcification in the benthic community is significant (Martin et al., 2007a, 2007b) and directly impacts A_T. For spring we can express the observed ratio in terms of the empirical changes induced by these two processes (OM production and calcification):

$$1.(\Delta AT:\Delta DIC\ (0.36)) = x.(17/106) - y.(2/1), \qquad \text{(Eq. 8)}$$

where x and y represent the proportion of change in DIC and A_T of each of these processes (adding up to 1, or 100%). Solving this equation indicates that changes in the ΔAT:ΔDIC ratio are 89% driven by OM production (by pelagic and benthic communities) and 11% driven by calcification. During early spring, the observed anomaly in A_T indicates a source of A_T in the Bay of Brest (Fig. 7b). Using monthly averaged changes, an average of 65% of the change in A_T concentration in spring can be attributed to NO_3^- uptake by pelagic phytoplankton.

Further, there are a number of processes, which generate A_T in the coastal benthic environment (e.g. sulfate reduction, and nitrification), however, such reactions only take place under anoxic conditions and the *Maerl* communities which dominate the Bay of Brest are well-oxygenated (Martin et al., 2007b). Annually, the A_T source reaches a peak of ~30 µmol kg^{-1}. Similar changes in A_T in Liverpool Bay have been attributed to PP over the spring period (Hydes and Hartman, 2012), indicating the A_T source is a result of OM production. In the Bay of Brest, the measured peaks in calcification rate of the benthic community (Martin et al., 2007a) coincide with the two observed peaks in annual A_T distribution shown here (Fig. 2f). It has been calculated that the *Maerl* beds in the Bay of Brest can contribute to more than half of the annual PP of the Bay, with an annual gross community production up to 2 times higher than that of the phytoplankton community (Martin et al., 2007a). These authors also show that PP in the Maerl community largely exceeds the $CaCO_3$ production. As such, we propose that the observed peaks in A_T stem predominantly from the PP performed by the benthic community.

During summer the ratio of ΔAT:ΔDIC reaches a minimum of 0.26. In summer OM production is still high, with rates of 111 mg C m^{-2} day^{-1} (Ní Longphuirt et al., 2007), thus if we assume that biology is still the dominant process impacting A_T, then the summer ratio indicates that 95% of the changes are effected by OM production/remineralisation and 5% by calcification. As previously mentioned, the NCP_{summer} is closely related to the amount of production previously carried out, and therefore at this time of year both production and remineralisation are occurring simultaneously in the Bay.

The *Maerl* communities in the Bay of Brest support a large population of *C. fornicata* and red coral, all of which perform calcification (Chauvaud et al., 2000; Martin et al., 2006; Longphuirt et al., 2007) and summertime marks the peak in $CaCO_3$ precipitation in the *Maerl* communities in the Bay, with rates of 4.2 mmol $CaCO_3$ m^{-2} h^{-1} (Martin et al., 2007a). After mid-spring the component $A_T|_{OMP}$ changes sign and the Bay of Brest presents a sink of A_T (Fig. 7b), which is consistent with calcification. With the increase in calcification one would expect to see an increase in ΔAT:ΔDIC ratios, not a decrease, as is observed, and the observed A_T:DIC ratio (Figure 4d) shows a peak, in accordance with calcification. The negative NCP observed at this time of year, and the aforementioned recovery of $Si(OH)_4$ concentrations show that a notable amount of remineralisation is taking place, in both the pelagic and benthic compartments. Nitrification is thus a likely process and we suggest that the remineralisation signal is sufficiently large to mask the benthic calcification signal resulting in the observed low ΔAT:ΔDIC ratio.

During autumn the ΔAT:ΔDIC ratio returns to the same value observed in spring: 0.36. This is caused by increasing DIC and A_T values, with $A_T|_{OMP}$ values indicating an unaccounted for source of A_T (Fig. 7b). Martin et al. (2007a) found that community respiration did not vary notably between spring and autumn, thus the autumn ratio is likely to indicate the inverse processes of spring: OM remineralisation and calcium carbonate dissolution. As previously quoted, this ratio results in 11% of changes in A_T and DIC being attributed to $CaCO_3$ dissolution, which is within the range quoted by Krumins et al. (2013). These authors found that particulate inorganic carbon (PIC) dissolution accounts for 9-19% of generated A_T in carbonate shelf sediments (19% in Bay environments). The particulate organic carbon (POC) flux to the sea floor has a direct impact on this dissolution through the release of CO_2 from remineralisation and the associated concomitant decrease in pH (Morse & Mackenzie, 1990; Krumins et al., 2013). As such, one would expect in years of greater production there would be a greater amount of dissolution in autumn or winter, which would manifest in the A_T source. However, only minor variations in this $A_T|_{OMP}$ source (Fig. 7b) are seen between years and minimum winter pH values do not show any relationship to the size of the A_T sink/source nor to the spring and summer NCP. In autumn the freshwater flux into the Bay of Brest increases and we suggest that the increased flushing time of waters in the Bay prevent the spring and summer signal from manifesting in autumn, and subsequently, winter.

In summary, the carbonate system in the Bay of Brest is strongly dictated by the benthic community in the Bay of Brest, and shows surprisingly little variation between years. Biological processes exert a dominant influence from spring through to summer, as has been found in the adjacent Celtic and Irish Seas and the western

English Channel (Marrec et al., 2015). The seasonal ratios between DIC and A_T remain stable between years, indicating a regulated balance between OM production and calcification. The benthic compartment exerts a strong influence on the pelagic signal in spring and summer, particularly with regard to A_T distribution. As previously stated, the spring nutrient concentrations exert a strong control over the spring and summer NCP and the spring air-sea CO_2 flux. The close link between these two environments has been previously noted (Le Pape et al., 1999; Del Amo, 1997), and is likely related to the *silicic acid pump*. This mechanisms has previously been suggested to give the Bay a resilience to eutrophication, by regulating the levels of PP. We suggest that the same mechanism will help to limit and regulate the carbonate system, and as such, the main drivers of CO_2 variability in the Bay of Brest would be river nutrient contributions and the physical factors controlling air-sea CO_2 flux (e.g. temperature and wind-speed).

5.3 Net Community Production and Air-Sea Flux of CO_2

The North Atlantic water fraction dominates the carbon budget in the Bay of Brest, representing between 82 – 99% throughout the year (based on salinity). The Bay is, on average, heterotrophic on an annual basis, acting as a source of CO_2 to the atmosphere. The NCP is the dominant carbon sink in the Bay of Brest, whereas variation in river DIC contribution is, on yearly average, just 2.5% of the variation accountable to NCP. For most years, the direction of the spring air-sea CO_2 flux dominates the annual trend and thus determines whether the Bay behaves as an annual source or sink of CO_2 to the atmosphere.

Calculated NCP values show a trend of negative values (indicative of PP>CR) throughout autumn and winter, switching to positive values in spring. Summer NCP shows a general shift back to negative values, although closer to zero than winter values. Thus during late spring - early summer the shift from an autotrophic system to a heterotrophic one occurs. The reversal of the NCP sign accompanies the onset of the decline in Chl-*a* concentrations and the increase in pCO_2 values. It has been described that post nutrient-exhaustion in the Bay, climatic variability controls pelagic primary production (Quéguiner and Tréguer, 1984), and thus during summer the effect of temperature on CO_2 solubility exerts greater affect than biological processes on air-sea fluxes (Bozec et al., 2011). The same switch is observed in the southern North Sea, a similar shallow, coastal ecosystem, whereby under-saturation of CO_2 in springtime gives way to super-saturation of CO_2 in summertime caused by the decoupling of production and respiration (Thomas et al., 2004). The switch from biological to physical controls explains why the NCP_{summer}, which is related to NCP_{spring}, does not express the same relationship with air-sea CO_2 flux, and results in an air-sea CO_2 flux of ~0 for all years. The consistency of this zero flux between years is indicative of the small variability observed in summertime temperatures between years. In autumn and winter the effects of wind speed and fresh water fluxes obscure the influence of NCP on pCO_2 fluxes (Bozec et al., 2011).

The calculated spring NCP values (19 – 78 mg C m^{-2} d^{-1}) are of a similar order of magnitude to those reported by Ní Longphuirt et al. (2007), in the pelagic zone, during the spring bloom (79 mg C m^{-2} d^{-1}). Our values are somewhat more conservative to those of Del Amo et al. (1997) calculated for the pelagic zone in summer (286 mg C m^{-2} d^{-1}). The latter authors both used average measured daily

values in March and May to represent the season, whereas our total seasonal NCP was divided by the number of days to obtain a daily average. In spring we observe significant differences in NCP between the months of March and May, in addition to variability between years. Similarly, considerable inter-annual variability in primary NCP has previously been noted in the Bay of Brest, by Del Amo et al. (1997).

The direct link between the biological pump and the physical pump (whereby the CO_2 deficit created by biological uptake is replaced via the physical pump) is often apparent in significant relationships between NCP and air-sea CO_2 flux, which has been found in coastal and oceanic environments (Calleja et al., 2005; Lockwood et al., 2012). During spring the Bay of Brest acts as a sink to atmospheric CO_2 for most years, and the size of the spring, and annual, CO_2 sink shows a significant correlation to the calculated spring NCP values (Fig. 9c) in line with the findings of Bozec et al. (2011); that in spring biological processes exert the preponderant influence over pCO_2 dynamics. Thus more negative CO_2 fluxes coincide with lower, or more negative, values of NCP. If we look at our NCP computations with monthly resolution (data not shown), we observe significant differences in NCP between the months of March (end of winter/beginning of spring) and April/May (Spring): March is the only month when the trend between NCP and CO_2 flux shows a negative linear relationship of higher NCP with more negative air-sea flux of CO_2 (as opposed to what we observe on Fig. 9c for the rest of Spring). The March relationship is statistically significant ($r=0.86$, p-value<0.05), and the ratio between NCP:air-sea CO_2 flux is 1:3.3. The ratio (3.3) is directly comparable to bloom regions in the northeast Pacific ocean (3.3), and the highly productive SubArctic region (2.8) of the Pacific (Lockwood et al., 2012). As mentioned above, in April and May there is a distinct difference in the relationship

between monthly NCP and air-sea CO_2 flux, with higher NCP values coinciding with higher (more positive) CO_2 fluxes. We discuss possible underlying processes below.

Jiang et al. (2013) found in the adjacent Bay of Biscay, that years of greater nutrient entrainment from below the mixed layer depth resulted in greater spring NCP, however, coincided with lower spring air-sea CO_2 fluxes. This has been attributed to those years displaying higher temperatures caused by the North Atlantic Oscillation (NAO), which outcompeted the effects of greater PP (Dumousseaud et al., 2010). The inter-annual temperature differences we observe in the Bay of Brest are insufficient to cause the observed differences in air-sea CO_2 fluxes. As we have shown NCP_{spring} and NCP_{summer} to be directly linked to the winter time peak $Si(OH)_4$ concentration, we suggest that as a result of the presence of the *silicic acid pump*, the amount of $Si(OH)_4$ available post-spring bloom is directly dependent upon the amount of recycling that has taken place. It thus follows that higher values of NCP in April and May are also indicative of greater levels of OM turnover, which will increase surface water pCO_2 and decrease the air-sea CO_2 flux. A similar trend has been observed in the Southern Bight of the North Sea (Gypens et al., 2004), although, in the North Sea, the initial CO_2 drawdown is larger than the subsequent release by respiration. In the Bay of Brest, the disparity from March to these two latter months is sufficiently large to change the trend for the entire season of spring. This result reflects the complexity of ecosystems with multiple drivers.

The annual air-sea flux of CO_2 shows significant variability, however generally acts as a source of CO_2 to the atmosphere. This is similar to a number of other shelf seas at

temperate latitudes, e.g. the southern North Sea (-0.33 – 0.22 mol C m^{-2} yr^{-1}; Sciettecatte et al., 2007), and the Scotian Shelf (1.4 mol C m^{-2} yr^{-1}; Shadwick et al., 2011), which is in contrast to the general classification of Chen and Borges, (2009). In the Bay of Brest, springtime is consistently a significant sink for atmospheric CO_2, whereas wintertime represents a more substantial source of CO_2 to the atmosphere. This balance, determined by wind speeds, temperature and NCP, has been found to tend to the other direction in the adjacent Bay of Biscay, with a wintertime air-sea flux of +3.7 mmol m^{-2} d^{-1} being outweighed by a summertime flux of -4.4 mmol m^{-2} d^{-1} (Dumoussead et al., 2010). While the Bay of Biscay has been determined a sink for CO_2 on numerous occasions, the size of the sink also shows inter-annual variability (Padin et al., 2009). Furthermore, within the English Channel, large spatial heterogeneity has been found based on physical structures (Marrec et al., 2013), leading to differences in air-sea fluxes of up to 0.5 mol C m^{-2} y^{-1}. Such results highlight the necessity of understanding the fundamental controls of each ecosystem to put any calculated fluxes into context.

The impact of large scale forcing on air-sea CO_2 fluxes, either directly, or indirectly, has been well documented in a number of shelf seas (Gonzalez-Davila et al., 2007; Gypens et al. 2011; Jiang et al., 2013). Gypens et al. (2011) found that in the southern Bight of the North Sea the inter-annual variability of air-sea CO_2 flux could be notably linked to net ecosystem production in addition to temperature and windspeeds. The results presented here show that in the Bay of Brest, due to the presence of the *silicic acid pump*, the annual NCP is heavily dependent upon the riverine supply of $Si(OH)_4$ to the Bay. In turn, there is a strong, significant correlation between NCP and annual air-sea CO_2 flux and, as such, the annual air-sea CO_2 flux is

indirectly controlled by riverine inputs, in addition to being directly impacted by temperature and windspeed (Bozec et al., 2011). The multi-faceted controls in the Bay of Brest, and in other similar shelf seas, makes it vital to fully understand the contribution of each factor and thus consider the impact of this decadal forcing when attempting to elucidate anthropogenic trends.

6 Concluding remarks

Based on a comprehensive dataset covering seven years of observations, the controls on the carbonate system in the Bay of Brest were found to vary over the annual cycle. During spring and summer, the DIC, A_T and pCO_2 distributions are heavily dominated by biological processes, which in turn are largely influenced by the *silicic acid pump* operating in the Bay. The spring and summer NCP is significantly correlated to the peak wintertime $Si(OH)_4$ concentrations, the former in concordance with a $Si(OH)_4$-limited system, the latter due to the recycling of biogenic silica following the initial spring bloom. However, the recycling, which liberates the $Si(OH)_4$ post-bloom, leads to elevated CO_2 concentrations and acts to reduce the sink of atmospheric CO_2 afforded by the Bay in late spring. The counter-intuitive relationship found between NCP and air-sea CO_2 flux presented here highlights the need for individual study of coastal environments, as such, a result would not have been predicted based on other findings in similar Bays or carbonate shelves.

Acknowledgements

SOMLIT-Brest and MAREL-Iroise are part of the IUEM Observatory (http://www-iuem.univ-brest.fr/observatoire/l-observatoire) and are supported by collaboration between IUEM/UBO, IFREMER and INSU. We thank the SOMLIT-Brest team from the IUEM for additional sampling of the carbonate system parameters. We are grateful to the SNAPO-CO_2 (Service National d'Analyse des paramètres Océaniques du CO_2) lab for assistance with the DIC/TA analysis. We thank M. Ramonet for providing the atmospheric CO_2 data from the RAMCES network (Observatory Network for Greenhouse gases). We thank two anonymous reviewers and the editor for their comments, which improved the quality of this manuscript. This work was supported by the French National program LEFE/INSU (CHANNEL project), the "Conseil Général du Finistère" (CG29) and the Région Bretagne (SAD program). Y.B. is P.I. of the CHANNEL project and Associate Researchers (CR1) at CNRS. L.S. holds a post-doctoral grant from CG29 and Région Bretagne.

References

Archer, D., 2005. Fate of fossil fuel CO_2 in geologic time. J. Geophys. Res. 110, C09S05. Doi:10.1029/2004JC002625.

Andersson, A. J., and Mackenzie, F. T., 2005. Shallow-Water Oceans: A Source of Sink of Atmospheric CO_2? Front. Evol. Environ. 2, 348-353.

Balch, W. M., Gordon, H. R., Bowler, B. C., Drapeau, D. T., and Booth, E. S., 2005. Calcium carbonate measurements in the surface global ocean based on Moderate-

Resolution Imaging Spectroradiometer data. J. Geophys. Res. 110, C07001. Doi:10.1029/2004JC002560.

Beucher, C., Tréguer, P., Corvaisier, R., Hapette, A. M., and Elskens, M., 2004. Production and dissolution of biosilica, and changing microphytoplankton dominance in the Bay of Brest (France). Mar. Ecol. Prog. Ser. 267, 57-69.

Borges, A. V., Delille, B., and Frankignoulle, M., 2005. Budgeting sinks and sources of CO2 in the coastal ocean: Diversity of ecosystems counts. Geophys. Res. Lett. 32, L14601. Doi:10.1029/2005GL023053.

Boutin, J. and Merlivat, L., 2009. New in-situ estimates of carbon biological production rates in the Southern Ocean from CARIOCA drifter measurements. Geophys. Res. Lett. 36, L13608. Doi: 10.1029/2009GL038307.

Bozec, Y., L. Merlivat, A.-C. Baudoux, L. Beaumont, S. Blain, E. Bucciarelli, T. Danguy, E. Grossteffan, A. Guillot, J. Guillou, M. Repecaud, P. Treguer (2011). Diurnal to inter-annual dynamics of pCO_2 recorded b a CARIOCA sensor in a temperate coastal ecosystem (2003-2009). Mar. Chem. 126:13-26. Doi:10.1016/j-marchem.2011.03.003.

Brewer, P.C. and Goldman, J.C., 1976. Alkalinity changes generated by phytoplankton growth. Limnol. Oceanogr. 21, 108-117.

Cai, W-. J., 2011. Estuarine and Coastal Ocean Carbon Paradox: CO_2 Sinks or Sites of Terrestrial Carbon Incineration? Annu. Rev. Mar. Sci. 3, 123-145.

Caldeira, K., and Wickett, M. E., 2005. Ocean model predictions of chemistry changes from carbon dioxide emissions to the atmosphere and ocean. J. Geophys. Res. 110, C09S04. Doi: 10.1029/2004JC002671.

Calleja, M. L., Duarte, C. M., Navarro, N., and Agusti, S., 2005. Control of air-sea CO_2 disequilibria in the subtropical NE Atlantic by planktonic metabolism under the ocean skin. Geophys. Res. Lett. 32, L08606. Doi:10.1029/2004GL022120.

Chauvaud, L., Jean, F., Ragueneau, O., and Thouzeau, G., 2000. Long-term variation of the Bay of Brest ecosystem: benthic-pelagic coupling revisited. Mar. Ecol. Prog. Ser. 200, 35-48.

Chen, C. -T. A, 1978. Decomposition of calcium carbonate and organic carbon in the deep oceans. Science, 201, 735-736.

Chen, C. -T. A, 2002. Shelf- vs. dissolution-generated alkalinity above the chemical lysocline. Deep-Sea Res. II 49, 5365-5375.

Chen, C. -T. A, and Borges, A.V. (2009). Reconciling opposing views on carbon cycling in the coastal ocean: continental shelves as sinks and near-shore ecosystems as sources of atmospheric CO_2. Deep Sea Res. II 33, L12603.

Clargo, N. M., Salt, L. A., Thomas, H., and de Baar, H.J.W., 2015. Rapid increase of observed DIC and pCO_2 in the surface waters of the North Sea in the 2001-2011 decade ascribed to climate change superimposed by biological processes. Mar. Chem. In Press.

Dee, D. P., Uppala, S. M., Simmons, A. J., Berrisford, P., Poli, P., Kobayashi, S., Andrae, U., Balmaseda, M. A., Balsamo, G., Bauer, P., Bechtold, P., Beljaars, A. C. M., van de Berg, L., Bidlot, J., Bormann, N., Delsol, C., Dragani, R., Fuentes, M., Geer, A. J., Haimberger, L., Healy, S. B., Hersbach, H., Holm, E. V., Isaksen, L., Kallberg, P., Kohler, M., Matricardi, M., McNally, A. P., Monge-sans, B. M., Morcrette, J. –J., Park, B., -K., Peubey, C., de Rosnay, P., Tavolato, C., THepaut, J., -N., and Vitart, F., 2011. The ERA-Interim reanalysis: configuration and performance of the data assimilation system, Q. J. R. Meteorol. Soc. 137, 553-597. Doi: 10.1002/qj.828.

Del Amo, Y., O. Le Pape, P. Treguer, B. Queguiner, A. Menesguen, A. Aminot (1997). Impacts of high-nitrate freshwater inputs on macrotidal ecosystems. I. Seasonal evolution of nutrient limitation for the diatom-dominated phytoplankton of the Bay of Brest (France). Mar. Ecol. Prog. Series. 161, 213-224.

Dickson, A.G. (1990). Standard potential of the reaction: AgCl(s) + 1/2H_2(g) = Ag(s) + HCl (aq), and the standard acidity constant of the ion HSO_4^- in synthetic seawater from 273.15 to 318.15K. J. Chem. Thermodyn. 22, 113-127.

Dickson, A.G., Sabine, C. L., and Christian, J. R. (Eds), 2007. Guide to Best Practices for Ocean CO_2 Measurements. PICES Special Publication 3.

Dumousseaud, C., E.P. Achterberg, T. Tyrrell, A. Charalampopoulou, U. Schuster, M. Hartman, and D.J. Hydes (2010). Contrasting effects of temperature and winter mixing on the seasonal and inter-annual variability of the carbonate system in the Northeast Atlantic Ocean. Biogeosciences, 7, 1481-1492.

Edmond, J., 1970. High Precision Determination of Titration Alkalinity and Total Carbon Dioxide Content of Sea Water by Potentiometric Titration. Deep Sea Res. and Oceanographic Abstracts 17, 737-750.

EPA, 1997. In vitro determination of chlorophyll a and pheophytin a in marine and freshwater algae by fluorescence (Arar E.J. & Collins G.B.). Method 445.0, revision 1.2. US-Environmental Protection Agency, Cincinnati, 26p.

Frankignoulle, M., and Borges, A. V., 2001. Direct and Indirect pCO_2 Measurements in a Wide Range of pCO2 and Salinity Values (The Scheldt Estuary). Aq. Geochem. 7, 267-273.

Gattuso, J. –P., Frankignoulle, M., and Wollast, R., 1998. Carbon and carbonate metabolism in coastal aquatic ecosystems. Annu. Rev. Ecol. Syst. 29, 405-433.

González-Dávila, M., J.M. Santana-Casiano, and E.F. Gonzalez-Davila (2007). Interannual variability of the upper ocean carbon cycle in the northeast Atlantic Ocean. Geophys. Res. Lett. 34:L07608. Doi:10.1029/2006g1028145.

Gypens, N., Lancelot, C., and Borges, A.V., 2004. Carbon dynamics and CO_2 air-sea exchanges in the eutrophied coastal waters of the Southern Bight of the North Sea: a modeling study. Biogeosciences, 1, 147-157. Doi:10.5194/bg-1-147-2004.

Gypens, N., Lacroix, G., Lancelot, C., and Borges, A.V., 2011. Seasonal and inter-annual variability of air-sea CO_2 fluxes and seawater carbonate chemistry in the Southern North Sea. Prog. Oceanogr. 88, 59-77.

Hydes, D.J., and Hartman, S.E., 2012. Seasonal and inter-annual variability in alkalinity in Liverpool Bay (53.5 N, 3.5 W) and in major river inputs to the North Sea. Oc. Dynamics. 62, 321-333. Doi: 10.1007/s10236-011-0503-7.

Jahnke, R. A, Craven, D.B., McCorkle, D.C., and Reimers, C.E. (1997). $CaCO_3$ dissolution in California continental margin sediments: The influence of organic matter remineralization. Geochim. Et Cosmochim. Acta 61, 3587-3604.

Jiang, Z.-P., D.J. Hydes, T. Tyrrell, S.E. Hartman, M.C. Hartman, C. Dumousseaud, X.A. Padin, I. Skjelvan, and C. Gonzalez-Pola (2013). Key controls on the seasonal and interannual variations of the carbonate system and air-sea CO2 flux in the Northeast Atlantic (Bay of Biscay). J. Geophys. Res. Oc. 118, 785-800, doi:10.1002/jgrc.20087.

Kalnay, E., Kanamitsu, M., Kistler, R., Collins, W., Deaven, D., Gandin, L., Iredell, M., Saha, S., White, G., Woollen, J., Zhu, Y., Leetmaa, A., Reynolds, R., Chelliah, M., Ebisuzaki, E., Higgins, W., Janowiak, J., Mo, K.C., Ropelewski, C., Wang, J., Jenne, R., Joseph, D., 1996. The NCEP/NCAR 40-year reanalysis project. Bull. Am. Meteorol. Soc. 77, 437-471.

Kitidis, V., Hardman-Mountford, N.J., Litt, E., Brown, I., Cummings, D., Hartman, S., Hydes, D., Fishwick, J.R., Harris, C., Martinez-Vicente, V., Malcolm, E., Woodward, S., and Smyth, T.J., 2012. Seasonal dynamics of the carbonate system in the Western English Channel. Cont. Shelf. Res. 42, 30-40.

Krumins, V., Gehlen, M., Arndt, S., van Cappellen, P., and Regnier, P., 2013. Dissolved inorganic carbon and alkalinity fluxes from coastal marine sediments: model estimates for different shelf environments and sensitivity to global change. Biogeosciences 10, 371-298.

Le Pape, O., Del Amo, Y., Menesguen, A., Aminot, A., Queguiner, B., and Treguer, P., 1996. Resistance of a coastal ecosystem to increasing eutrophic conditions: the Bay of Brest (France), a semi-enclosed zone of Western Europe. Cont. Shelf Res. 16, 1885-1907.

Le Pape, O., Jean, F., and Ménesguen, 1999. Pelagic and benthic trophic chain coupling in a semi-enclosed coastal system, the Bay of Brest (France): a modeling approach. Mar. Ecol. Prog. Ser. 189, 135-147.

Lefèvre, N., Ciabrini, J.P., Michard, G., Brient, B., DuChaffaut, M., and Merlivat, L., 1993. A new optical sensor for pCO_2 measurements in seawater. Mar. Chem. 42, 189-198.

Lewis, E. L. and Wallace, D. W. R., 1998. Program developed for CO_2 system calculations, ORNL/CDIAC-105, Carbon dioxide information analysis center, Oak Ridge National Laboratory, U.S. Department of Energy, Oak Ridge, 1998.

Lockwood, D., Quay, P.D., Kavanaugh, M.T., Juranek, L.W., and Feely, R.A., 2012. High-resolution estimates of net community production and air-sea CO_2 flux in the northeast Pacific. Global Biogeochem. Cyc. 26, GB4010. Doi:10.1029/2012GB004380.

Ni Longphuirt, S., Clavier, J., Grall, J., Chauvaud, L., Le Loc'h, F., Le Berre, I., Flye-Sainte-Marie, J., Richard, J., Leynaert, A., 2007. Primary production and spatial distribution of subtidal microphytobenthos in a temperate coastal system, the Bay of Brest, France. Est. Coast. and Shelf Sci. 74(3), 367-380.

Marrec, P., Cariou, T., Collin, E., Durand, A., Latimier, M., Macé, E., Morin, P., Raimund, S., Vernet, M., and Bozec, Y., 2013. Seasonal and latitudinal variability of the CO_2 system in the western English Channel based on Voluntary Observing Ship (VOS) measurements. Mar. Chem. 155, 29-41.

Marrec, P., Cariou, T., Latimer, M., Mace, E., Morin, P., Vernet, M., and Bozec, Y., 2014. Spatio-temporal dynamics of biogeochemical processes and air-sea CO_2 fluxes

in the Western English Channel based on two years of FerryBox deployment. J. Mar Syst. 140A, 26-38.

Marrec, P., Cariou, T., Mace, E., Morin, P., Salt, L.A., Vernet, M., Taylor, B., Paxman, K., and Bozec, Y., 2015. Dynamics of air-sea CO2 fluxes in the North-West European Shelf based on Voluntary Observing Ship (VOS) and satellite observations. Biogiosciences, In Press.

Martin, S., G. Thouzeau, L. Chauvaud, F. Jean, L. Guerin and J. Clavier (2006). Respiration, calcification, and excretion of the invasive slipper limpet, *Crepidula fornicata* L.: Implications for carbon, carbonate, and nitrogen fluxes in affected areas. Limnol. Oceanogr. 51: 1996-2007.

Martin, S., J. Clavier, L. Chauvaud, and G. Thouzeau (2007a). Community metabolism in temperate maerl beds. I. Carbon and carbonate fluxes. Mar. Ecol. Prog. Ser. 335: 19-29.

Martin, S., J. Clavier, L. Chauvaud, and G. Thouzeau (2007b). Community metabolism in temperate maerl beds. II. Nutrient fluxes, Mar. Ecol. Prog. Ser. 335: 31-41.

Middelburg, J.J., and Herman, P.M.J., 2007. Organic matter processing in tidal estuaries. Mar. Chem. 106, 127-147.

Millero, F.J., Graham, T.B., Huang, F., Bustos-Serrano, H., and Pierrot, D., 2006. Dissociation constants of carbonic acid in seawater as a function of salinity and temperature. Mar. Chem. 100, 80-94.

Milliman, J.D. and Droxler, A.W., 1996. Neritic and pelagic carbonate sedimentation in the marine environment: ignorance is not bliss. Geol. Rundsch. 85, 496-504.

Morse, J. W., and Mackenzie, F. T., 1990. Geochemistry of Sementary Carbonates, Elsevier, New York.

Nightingale, P.D., Malin, G., Law, C.S., Watson, A.J., Liss, P.S., Liddicoat, M.I., Boutin, J., Upstill-Goddard, R.C., 2000. In situ evaluation of air-sea gas exchange parameterizations using novel conservative and volatile tracers. Global Biogeochem. Cycles 14, 373-387.

Orr, J.C., Fabry, V.J., Aumont, O., Bopp, L., Doney, S.C. et al. 2005. Anthropogenic ocean acidification over the twenty-first century and its impact on calcifying organisms. Nature 437, 681-686.

Otero, P., Padin, X.A., Ruiz-Villarreal, M. –R., García-García, L. M., Ríos, A. F., and Perez, F. F. 2013. Net sea-air CO2 flux uncertainties in the Bay of Biscay based on the choice of wind speed products and gas transfer parameterizations. Biogeosciences 10, 2993-3005. Doi: 10.5194/bg-10-2993-2013.

Padin, X.A., G. Navarro, M. Gilcoto, A.F. Rios, and F.F. Perez (2009). Estimation of air-sea CO2 fluxes in the Bay of Biscay based on empirical relationships and remotely sensed observations. J. Mar. Syst. 75: 280-289. Doi: 10.1016/j.marsys.2008.10.008.

Quay, P.D., and Stutsman, J., 2003. Surface layer carbon budget for the subtropical N. Pacific: ∂^{13}C constraints at station ALOHA. Deep Sea Res. 50, 1045-1061. Doi. 10.1016/S0967-0637(03)00116-X.

Quéginer, B. and Tréguer, P., 1984. Studies on the Phytoplankton in the Bay of Brest (Western Europe). Seasonal Variations in Composition, Biomass and Production in Relation to Hydrological and Chemical Features (1981-1982). Botanica Marina, XXVII, 449-459.

Ragueneau, O., Chauvaud, L., Leynaert, A., Thouzea, G., Paulet, Y., Bonnet, S., Lorrain, A., Grall, J., Corvaisier, R., Hir, M.L. and Clavier, J., 2002. Direct evidence

of a biologically active coastal silicate pump: Ecological implications. Limnol. Oceanogr. 47, 1849-1854.

Ragueneau, O., Chauvaud, L., Moriceau, B., Leynaert, A., Thouzea, G., Donval, A., Le Loc'h, F., and Jean, F., 2005. Biodeposition by an invasive suspension feeder impacts the biogeochemical cycle of Si in a coastal ecosystem (Bay of Brest, France). Biogeochemistry, 75, 19-41. Doi: 10.1007/s10533-004-5677-3.

Ribas-Ribas, M., Rerolle, V.M.C., Bakker, D.C.E., Kitidis, V., Lee, G.A., Brown, I., Achterberg, E.P., Hardman-Mountford, N.J., and Tyrrell, T., 2014. Intercomparison of carbonate chemistry measurements on a cruise in northwestern European shelf seas. Biogeoscienes. 11, 4339-4355. Doi:10.5194/bg-11-4339-2014.

Sakamoto, A., Watanabe, Y.W., Osawa, M., Kido, K., Noriki, S., 2008. Time series of carbonate system variables off Otaru coast in Hokkaido, Japan. Est. Coast Shelf Sci. 79, 377-386.

Salt, L.A., Thomas, H., Borges, A., Bozec, Y., and de Baar, H.J.W., 2015. The Internal Consistency of the North Sea Carbonate System. J. Mar. Syst. In Press.

Sabine, C.L., R.A. Feely, N. Gruber, R.M. Key, K. Lee, J.L. Bullister, R. Wanninkhof, C.S. Wong, D.W.R. Wallace, B. Tilbrook, F.J. Millero, T.-H. Peng, A.

Kozyr, T. Ono and A.F. Rios (2004). The Oceanic Sink for Anthropogenic CO_2. *Science* 305, 367-371.

Sarmiento, J. L., and Gruber, N., 2006. Ocean biogeochemical dynamics, Cambridge University Press, 2006.

Schoemann, V.S, Becquevort, S., Stefels, J., Rousseau, V., and Lancelot, C., 2005. Phaeocystis blooms in the global ocean and their controlling mechanisms: A review. J. Sea Res. 53, 43-66.

Sciettecatte, L. –S., Thomas, H., Bozec, Y., and Borges, A. V., 2007. High temporal coverage of carbon dioxide measurements in the Southern Bight of the North Sea. Mar. Chem. 106, 161-173.

Shadwick, E. H., Thomas, H., Azetu-Scott, K., Greenan, B. J. W., Head, E., and Horne, E., 2011. Seasonal variability of dissolved inorganic carbon and surface water pCO_2 in the Scotian Shelf region of the Northwestern Atlantic. Mar. Chem. 124, 23-37.

Thomas, H., Ittekkot, V., Osterroht, C., and Shneider, B., 1999. Preferential recycling of nutrients: The ocean's way to increase new production and to pass nutrient limitation? Limnol. Oceanogr. 44, 1999-2004.

Thomas, H., Bozec, Y., Elkalay, K., de Baar, H. J. W., Borges, A. V., and Sciettecatte, L. –S., 2005. Controls of the surface water partial pressure of CO_2 in the North Sea. Biogeosciences 2, 323-334.

Tréguer, P., E. Goberville, N. Barrier, S. L'Helguen, P. Morin, Y. Bozec, P. Rimmelin-Maury, M. Czamanski, E. Grossteffan, T. Cariou, M. Répécaud, and L. Quéméner (2014). Large and local-scale influences on physical and chemical characteristics of coastal waters of Western Europe during winter. J. Mar. Syst. 139: 79-90. Doi: 10.1016/j.marsys.2014.05.019.

Tsunogai, S., Watanabe, S., and Sato, T., 1999. Is there a "continental shelf pump" for the absorption of atmospheric CO_2? Tellus S. B. 51, 701-712.

Weiss, R.F., 1970. Solubility of nitrogen, oxygen and argon in water and seawater. Deep Sea Res. 17, 721-735.

Weiss, R.F., and Price, B.A., 1980. Nitrous oxide solubility in water and seawater. Mar. Chem. 8, 347-359.

Wolf-Gladrow, D. A., Zeebe, R. E., Klaas, C., Kortzinger, A., and Dickson, A. G., 2007. Total alkalinity: The explicit conservative expression and its application to biogeochemical processes. Mar. Chem. 106, 287-300.

Wollast, R., 1998. Evaluation and comparison of the global carbon cycle in the coastal zone and in the open ocean. In Brink, K.H. and Robinson, A. R. (Eds), The Global Coastal Ocean, Volume 10. John Wiley & Sons, New York.

Figure Captions

Figure 1. Location of the Bay of Brest on the northwest Atlantic shelf. The red dots indicate the SOMLIT-Brest sampling station, and the MAREL-Iroise buoy (equipped with the pCO_2 CARIOCA sensor), located 100m offshore from here. The green dot represents the sampling station *Roscanvel*, a region representative of the Bay of Brest where calcification was measured from March 2002 to October 2004 (Martin et al., 2006). The two main rivers of the Bay of Brest, the Elorn and the Aulne, are also shown.

Figure 2. Calculated climatological monthly values for the period of 2008 to 2014 of (a) salinity and temperature (°C), (b) chlorophyll-*a* (µg L^{-1}) and dissolved oxygen saturation (DO%), (c) pH and pCO_2 (µatm), (d) flow rate of the rivers Elorn and Aulne (m^3 $month^{-1}$), (e) concentrations of nitrate and silicate (µmol kg^{-1}) and (f) DIC and A_T (µmol kg^{-1}). Data shown in panels (a), (b), (c), are climatologies based on high-frequency data collected at the MAREL-Iroise site. The river flow climatologies

(d) are based on daily measurements available at http://www.hydro.eaufrance.fr/. Data shown in panels (e) and (f) are based on weekly measurements at the SOMLIT station. The monthly values are displayed with one standard deviation of their variability.

Figure 3. Monthly averaged time series measurements of (a) salinity, temperature (°C), (b) flow rate of the rivers Elorn and Aulne (m^3 $month^{-1}$), (c) concentrations of nitrate and silicate (µmol kg^{-1}), (d) chlorophyll-*a* (µg L^{-1}) and pCO_2 (µatm), and (e) DIC and A_T (µmol kg^{-1}). The data displayed here are the same as those used to calculate the climatological values displayed in Fig. 2.

Figure 4. For the period 2008-2014, winter regressions of (a) salinity against DIC, and (b) salinity against A_T, and (c) Annual relationship of DIC with A_T in winter, spring, summer and autumn. The changes due to calcium carbonate precipitation and dissolution, organic matter production and remineralisation and air-sea gas exchange are marked on as vectors.

Figure 5. The monthly average contribution of the three main factors controlling DIC distribution ($DIC|_{NCP}$, $DIC|_{TRSP}$, and $DIC|_{EX}$) plotted with observed DIC ($DIC|_{OBS}$) in µmol DIC kg^{-1}.

Figure 6. (a) Monthly average A_T concentrations marked on the same plot as the predicted A_T based on the wintertime salinity-A_T regression. (b) Difference between this predicted A_T (based on salinity-A_T winter regression) and the observed A_T ($A_{T|OBS}$) in µmol A_T kg^{-1}.

Figure 7. Calculated, total seasonal air-sea CO_2 fluxes for each year (mol C m^{-2}), grouped by season over the 2008-2014 period.

Figure 8. Relationship between seasonal NCP values (NCP_{spring} and NCP_{summer}) and (a) peak wintertime silicate concentration, (b) nitrate concentration, and (c) seasonal air-sea CO_2 fluxes (shown regression has r value of -0.91 (p-value: 0.012), and (d) NCP_{spring} and NCP_{summer}, over the 2008-2014 period using the NCP computed in table 2.

Table Captions

Table 1. Seasonal, zero-salinity end members for A_T and DIC (both in µmol kg^{-1}) in the rivers Aulne and Elorn. The approximate contribution (%), based on salinity and flow rate climatologies, of each of these rivers is included in brackets. The variance of the water mass fraction is calculated based on inter-annual river flow variability. The end members for the North Atlantic (Bay of Biscay) have also been given as an indication of seasonal variability.

Table 2. Calculated annual and seasonal NCP values (mol C m^{-2} y^{-1}).

Tables

Table 1. Measured seasonal, zero-salinity end members for A_T and DIC (μmol kg^{-1}) in the rivers Aulne and Elorn. The approximate contributions of the two rivers and the North Atlantic are given as a percentage (%) of the water budget, based on salinity measurements and flow rate climatologies of each river. The variance of the water mass fraction is calculated based on inter-annual river flow variability and salinity of each season.

Season	**Aulne**			**Elorn**			**North Atlantic (Bay of Biscay)***		
	A_T, S=0	**DIC, S=0**	**% water mass**	**A_T, S=0**	**DIC, S=0**	**% water mass**	**A_T, S=35**	**DIC, S=0**	**% water mass**
Winter	257	341	3.4 ± 2.0	510	541	0.7 ± 0.3	2340*	2121*	96±2
Spring	297	381	3 ± 0.9	376	444	0.8 ± 0.3	-	-	96±2
Summer	305	360	1.4 ± 0.2	443	484	0.6 ± 0.2	2350*	2063*	98±1
Autumn	257	341	0.7 ± 0.4	510	541	0.3 ± 0.2	-	-	99±1

*Average values taken from Dumousseaud et al., 2010, representing the Northern Bay of Biscay.

Table 2. Calculated annual and seasonal NCP values (mol C m^{-2} y^{-1}) as per Eq. 3 in section 3.2.2. Seasons missing two months of data were not included, however, seasons missing one month of data were supplemented with the appropriate climatological, monthly average NCP value. Years missing one season of data were supplemented with the calculated seasonal average from all other years.

Year	Winter (Dec-Feb)	Spring (Mar-May)	Summer (Jun-Aug)	Autumn (Sep-Nov)	Annual
2008	N/A	N/A	N/A	-0.10	N/A
2009	-0.12	-0.51	N/A	-0.27	0.83
2010	N/A	0.24	0.33	0.17	-0.58
2011	-0.08	-0.19	0.17	-0.25	0.41
2012	-0.24	-0.14	0.36	N/A	0.12
2013	N/A	-0.49	0.13	-0.26	1.34
2014	-0.98	-0.56	0.07	-0.24	1.09

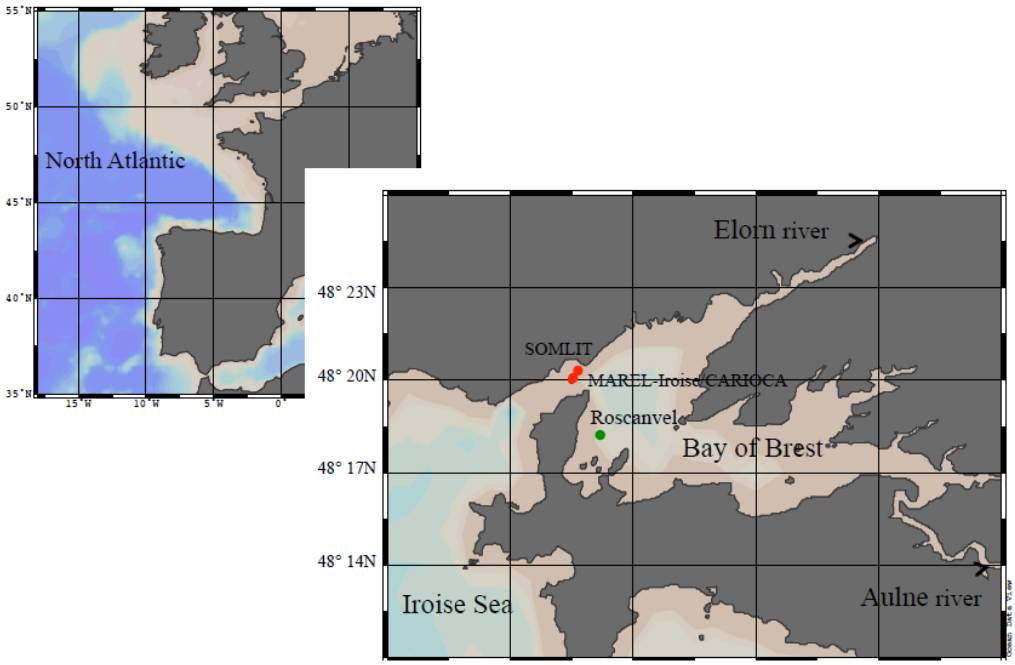

Figure 1

Figure 2

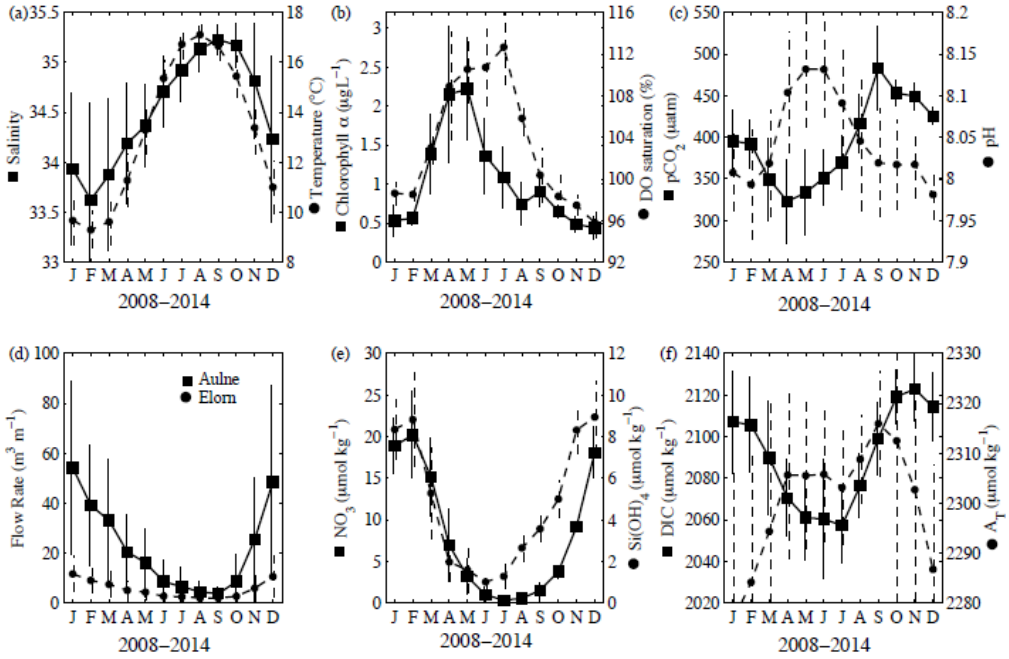

Figure 3

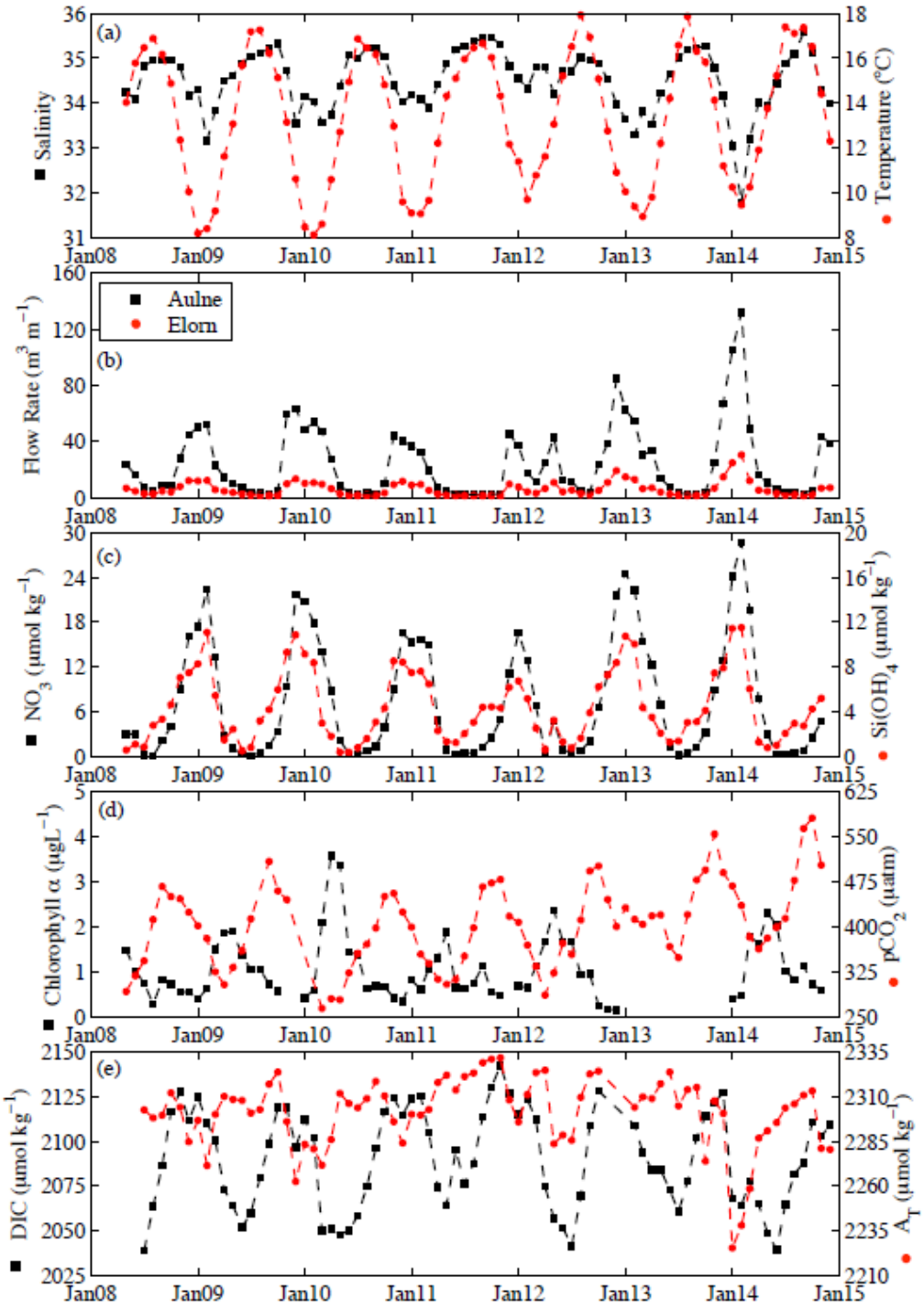

Figure 4

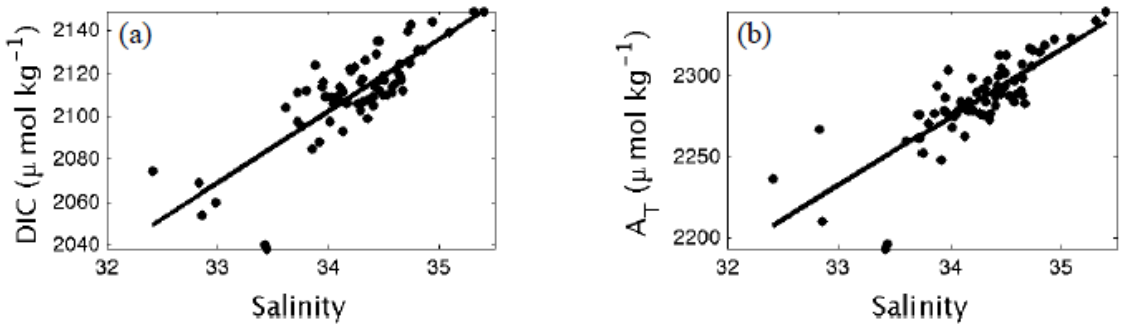

Figure 5

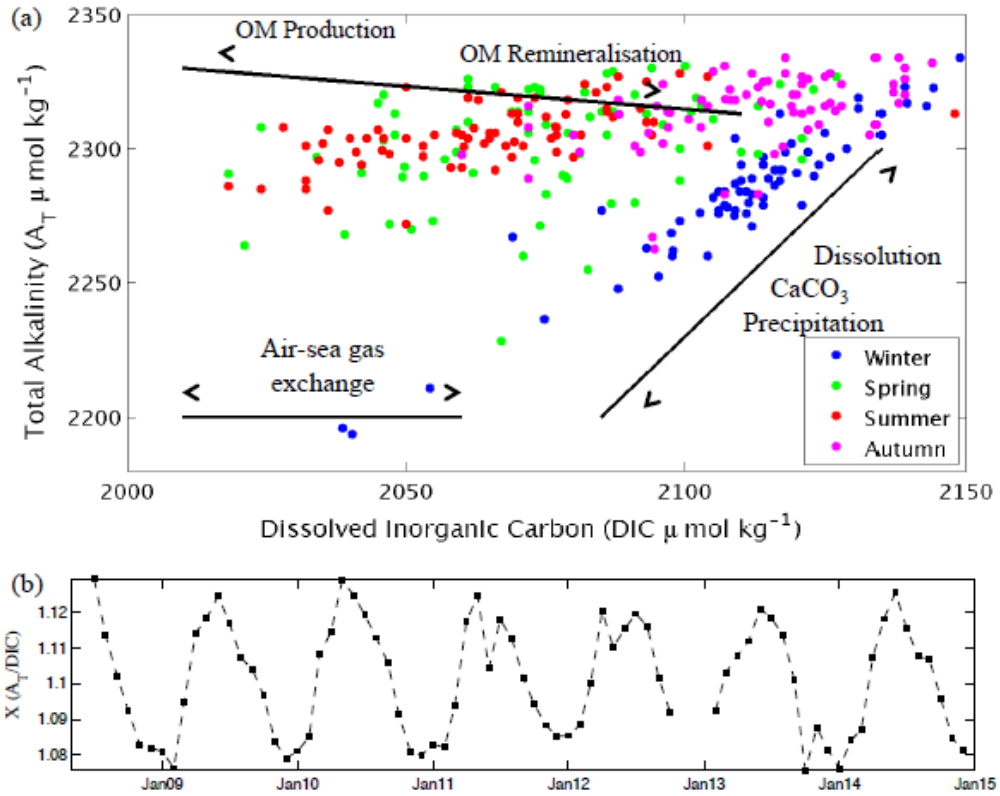

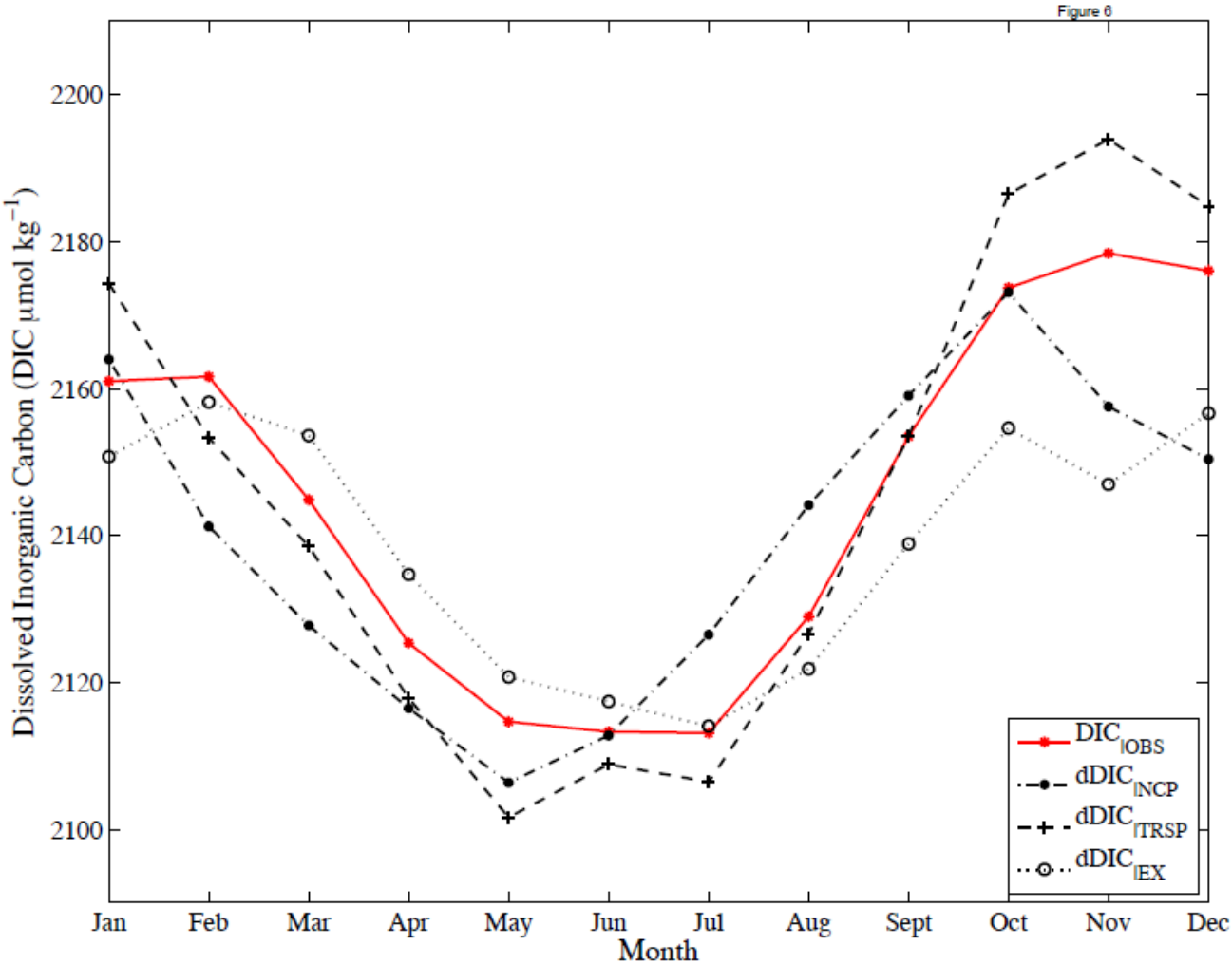

Figure 7

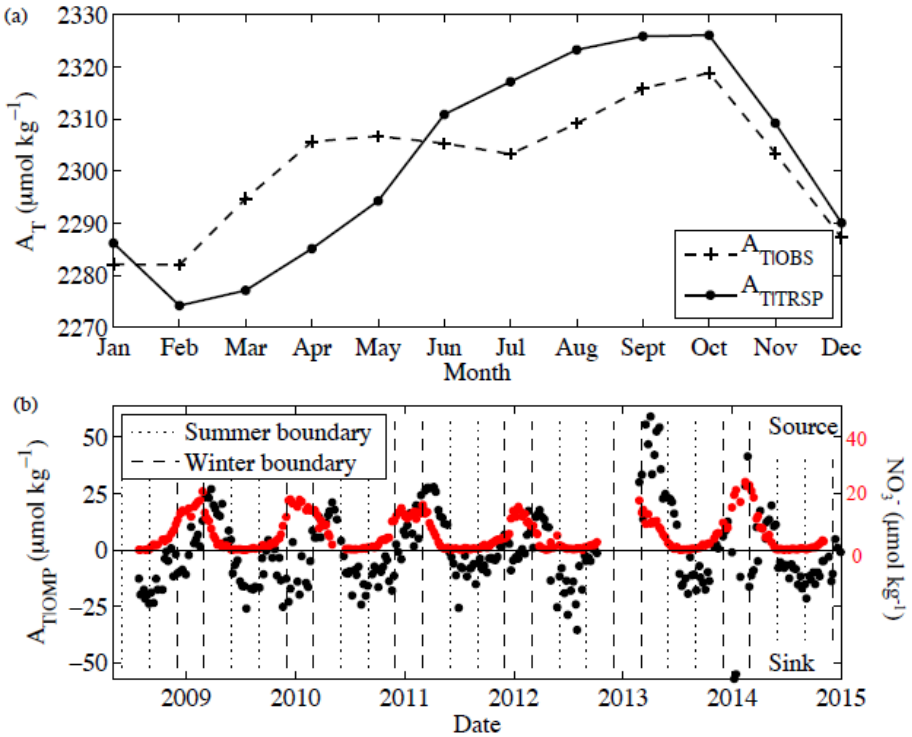

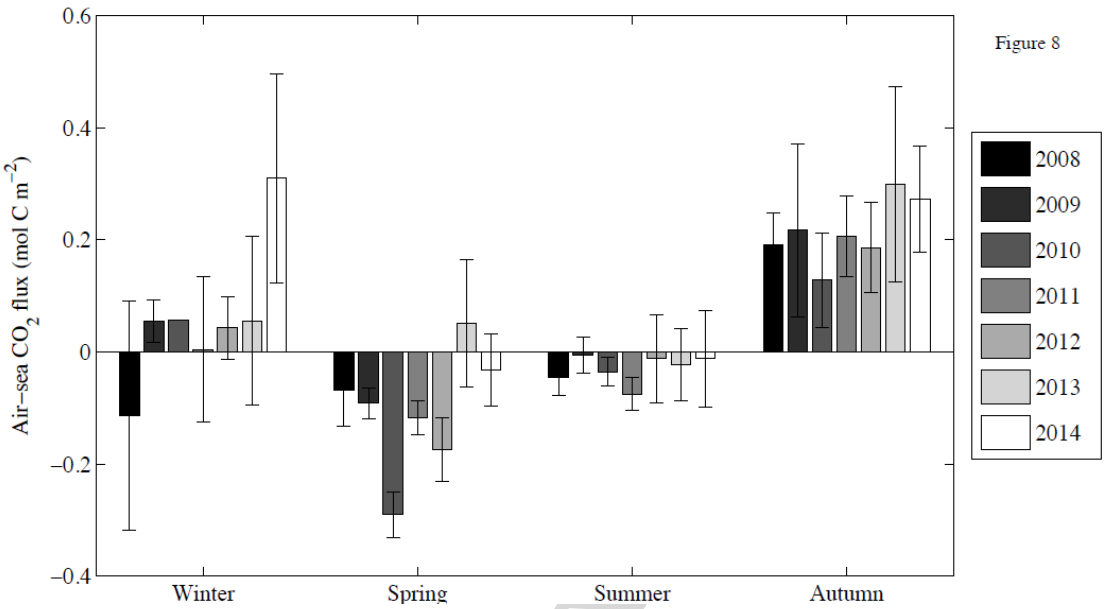

Figure 9